

พยาธิกลไกในการเกิดโรคกระดูกพรุนชนิดที่ถ่ายทอดโดยโครโมโซมเอ็กซ์



นางสาวศิริประภา ทองกอบเพชร

จุฬาลงกรณ์มหาวิทยาลัย

บทคัดย่อและแฟ้มข้อมูลฉบับเต็มของวิทยานิพนธ์ตั้งแต่ปีการศึกษา 2554 ที่ให้บริการในคลังปัญญาจุฬาฯ (CUIR)

เป็นแฟ้มข้อมูลของนิสิตเจ้าของวิทยานิพนธ์ ที่ส่งผ่านทางบัณฑิตวิทยาลัย

The abstract and full text of theses from the academic year 2011 in Chulalongkorn University Intellectual Repository (CUIR) are the thesis authors' files submitted through the University Graduate School.

วิทยานิพนธ์นี้เป็นส่วนหนึ่งของการศึกษาตามหลักสูตรปริญญาวิทยาศาสตรดุษฎีบัณฑิต

สาขาวิชาชีวเวชศาสตร์ (สหสาขาวิชา)

บัณฑิตวิทยาลัย จุฬาลงกรณ์มหาวิทยาลัย

ปีการศึกษา 2560

ลิขสิทธิ์ของจุฬาลงกรณ์มหาวิทยาลัย

PATHOMECHANISM OF X-LINKED OSTEOGENESIS IMPERFECTA

Miss Siraprapa Tongkobpetch



A Dissertation Submitted in Partial Fulfillment of the Requirements  
for the Degree of Doctor of Philosophy Program in Biomedical Sciences  
(Interdisciplinary Program)

Graduate School

Chulalongkorn University

Academic Year 2017

Copyright of Chulalongkorn University



ศิริประภา ทองกอบเพชร : พยาธิกลไกในการเกิดโรคกระดูกเปราะชนิดที่ถ่ายทอดโดยโครโมโซม  
 เอ็กซ์ (PATHOMECHANISM OF X-LINKED OSTEOGENESIS IMPERFECTA) อ.ที่ปรึกษา  
 วิทยานิพนธ์หลัก: ศ. นพ. วรศักดิ์ โชติเลอศักดิ์, อ.ที่ปรึกษาวิทยานิพนธ์ร่วม: ศ. ดร. พญ. กัญญา สุก  
 ปิติพร, 75 หน้า.

โรคกระดูกเปราะเป็นโรคพันธุกรรมที่ระบุได้จากความผิดปกติของรูปร่างกระดูกและการหักซ้ำของ  
 กระดูกหลายครั้ง คณะผู้วิจัยได้ค้นพบยีน *MBTPS2* ว่าเป็นยีนก่อโรคกระดูกเปราะที่มีการถ่ายทอดผ่าน  
 โครโมโซมเอ็กซ์ โปรตีน MBTPS2 หรือ S2P เป็นเอนไซม์ที่ทำหน้าที่ในการตัดโปรตีนที่ฝังตัวอยู่ในเมมเบรน  
 เมื่อโปรตีนที่ฝังตัวอยู่ในเมมเบรนถูกตัด โปรตีนเหล่านี้จะทำหน้าที่ควบคุมการสร้างของยีนอื่น ๆ คณะผู้วิจัย  
 ตรวจสอบว่าการกลายพันธุ์ที่พบในยีน *MBTPS2* มีผลกระทบกับการทำงานของโปรตีน S2P โดยตรวจสอบการ  
 สร้างโปรตีนทั้งในระดับอาร์เอ็นเอและโปรตีน พบว่าการกลายพันธุ์ไม่มีผลกระทบกับการสร้างโปรตีน แต่พบว่า  
 ความสามารถในการตัดโปรตีนเป้าหมายลดลง โปรตีน ATF6 และ CREB3L1 เป็นโปรตีนเป้าหมายของ S2P  
 คณะผู้วิจัยพบว่าความสามารถในการทำหน้าที่ควบคุมการสร้างยีน *ATF6* ลดลง ส่วนโปรตีน CREB3L1 พบว่า  
 ปริมาณของโปรตีน CREB3L1 ที่ถูกตัดโดย S2P ลดลง ทั้งสองส่วนนี้แสดงให้เห็นว่าการกลายพันธุ์ส่งผลให้  
 ความสามารถในการตัดโปรตีนเป้าหมายของ โปรตีน S2P ลดลง นอกจากนี้คณะผู้วิจัยได้ทำการศึกษา  
 กระบวนการเกิดโรคของโรคกระดูกเปราะที่ถ่ายทอดผ่านโครโมโซมเอ็กซ์ที่มีการกลายพันธุ์ในยีน *MBTPS2*  
 คณะผู้วิจัยได้สร้างเซลล์ที่มีลักษณะคล้ายเซลล์ต้นกำเนิดจากไฟโบรบลาสต์ที่ได้จากเซลล์ผิวหนังของผู้ป่วย และ  
 ทำการเหนี่ยวนำเซลล์ดังกล่าวให้เป็นออสทีโอเบลาสต์ ในกระบวนการสร้างออสทีโอเบลาสต์คณะผู้วิจัยพบว่า  
 ขั้นตอนการฝังตัวของแคลเซียมเกิดความล่าช้าหรือไม่พบการฝังตัวของแคลเซียมและพบความผิดปกติของ  
 รูปแบบการฝังตัวของแคลเซียมในเซลล์ที่ได้จากผู้ป่วย รวมไปถึงการศึกษาการแสดงออกของยีนระหว่างการสร้าง  
 ออสทีโอเบลาสต์แสดงความผิดปกติส่งผลถึงการสร้างออสทีโอเบลาสต์และกระบวนการฝังตัวของแร่ธาตุเพื่อ  
 สร้างความแข็งแรงให้กระดูก ผลดังกล่าวสนับสนุนความผิดปกติที่พบในกระบวนการฝังตัวของแคลเซียม  
 คณะผู้วิจัยยังค้นพบการแสดงออกที่ลดลงของกลุ่มยีน *COL1A1 SPARC SEC23A SEC24D* และ *LOX* กลุ่มยีน  
 ดังกล่าวมีความเกี่ยวข้องกับกระบวนการสร้างกระดูก โดยยีน *COL1A1* เป็นยีนที่ถูกควบคุมการสร้างโดยโปรตีน  
 CREB3L1 ส่วนยีนอื่น ๆ ในกลุ่มอาจถูกควบคุมการสร้างทั้งทางตรงและทางอ้อมโดยโปรตีน CREB3L3 จาก  
 ข้อมูลที่กล่าวมาสรุปได้ว่ากลไกการเกิดโรคกระดูกเปราะที่ถ่ายทอดผ่านโครโมโซมเอ็กซ์อาจเกิดจากความ  
 ผิดปกติในกระบวนการสร้างออสทีโอเบลาสต์และกระบวนการฝังตัวของแร่ธาตุเพื่อสร้างความแข็งแรงให้กระดูก  
 ซึ่งความผิดปกตินี้เป็นผลมาจากการทำงานที่ลดลงของกลุ่มยีน *COL1A1 SPARC SEC23A SEC24D* และ *LOX*  
 ที่ทำหน้าที่ในการสร้างกระดูก โดยกลุ่มยีนนี้ผ่านการควบคุมการสร้างจากโปรตีน CREB3L1 และ CREB3L3  
 ซึ่งเป็นโปรตีนเป้าหมายของโปรตีน S2P

สาขาวิชา ชีวเวชศาสตร์

ปีการศึกษา 2560

ลายมือชื่อนิติกร .....

ลายมือชื่อ อ.ที่ปรึกษาหลัก .....

ลายมือชื่อ อ.ที่ปรึกษาร่วม .....

# # 5487855420 : MAJOR BIOMEDICAL SCIENCES

KEYWORDS: MBTPS2 / CREB3L1 / CREB3L3 / X-LINKED OSTEOGENESIS IMPERFECTA

SIRAPRAPA TONGKOBPETCH: PATHOMECHANISM OF X-LINKED OSTEOGENESIS IMPERFECTA. ADVISOR: PROF. VORASUK SHOTELERSUK, M.D., CO-ADVISOR: PROF. KANYA SUPHAPEETIPORN, M.D., Ph.D., 75 pp.

Osteogenesis imperfecta (OI) or brittle bone disease is a genetic disorder characterized by deformities of bones and multiple bone fractures. We identified a new causative gene, *MBTPS2*, in two unrelated patients with OI inherited in X-linked pattern (X-OI). *MBTPS2* or site-2 protease (S2P) is a protease that cleaves the transmembrane proteins to activate them acting as transcription factors. To determine pathomechanism of X-OI caused by *MBTPS2* mutations, S2P functions were investigated. RNA and protein of S2P were stable. Instead, the defective S2P decreases its cleavage activities. ATF6 and CREB3L1 are target proteins of S2P. We demonstrated decreased transcriptional activity of ATF6 and a decreased transcription factor form of CREB3L1. Both of them were resulted from defects in the cleavage activity of S2P. In addition, we generated iPSCs from patients' skin fibroblasts and induced them to osteoblasts to elucidate the involving pathomechanism. During osteoblast differentiation, we found the delay or absence of calcium deposit and abnormal patterns of calcium binding in X-OI patients. Consistently, the studies of osteogenic gene expression revealed the defect of osteoblast differentiation and mineralization supporting the defects of calcium deposit. Interestingly, *COL1A1*, a downstream gene of CREB3L1, and *SPARC*, *SEC23A*, *SEC24D* and *LOX*, downstream genes of CREB3L3, were downregulated. These genes have functions involving in osteoblastogenesis. Taken together, we concluded that X-OI phenotype is possibly caused by the defects of osteoblast differentiation and mineralization resulting from the decreased transcriptional activities of CREB3L1 and CREB3L3 that downregulate *COL1A1*, *SPARC*, *SEC23A*, *SEC24D* and *LOX*.

Field of Study: Biomedical Sciences

Academic Year: 2017

Student's Signature .....

Advisor's Signature .....

Co-Advisor's Signature .....

## ACKNOWLEDGEMENTS

I would like to express my gratitude to everyone who participated in this work. First I am deeply grateful to my advisor, Prof. Vorasuk Shotelersuk for his patience, encouragement, motivation and suggestions of my PhD study. His guidance helped me in all the time of research and writing of this thesis. His advice on both research as well as on my lifestyle have been invaluable.

Besides my advisor, I would like to thank my co-advisor, Prof. Dr.Kanya Suphapeetiporn, and thesis committee: Prof. Dr.Apiwat Mutirangura, Assit. Prof. Dr. Rachaneekorn Tammachote, Prof. Dr.Sittisak Honsawek and Dr.Verayuth Praphanphoj for their insightful comments and encouragement.

My sincere thanks also goes to Dr.Ruttachuk Rangsiwiwat who provide me and opportunity to join his team. I would also like to thank all of the members of his team, especially Miss Wipawee Pavarajarn. Without their support, it would not be possible to conduct the stem cells for this research. I would like to thank Assit. Prof. Dr.Nipan Isarasena and his team for helps and suggestion.

Furthermore, I would like to thank everyone at the Center of Excellence for Medical Genetics, especially my lab mate, Miss Wandee Udomchaiprasertkul for the stimulating discussions, sharing knowledge, and working together. I would like to thank Ms. Kanyanut Thaweerachatham, Mr. Chalurmpon Srichomthong, Dr. Chupong Ittiwut, Dr. Rungnapa Ittiwut and Ms. Thivaratana Sinthuwiwat for all their support. And I really thank to my friends, Miss Jeeranan Jaiboonba and Miss Praweena Sinpitak, who help and support me all the time of my PhD student. Without their helps, my thesis would have been impossible to accomplish.

Finally, I would like to express my deepest gratitude to my family: parents, brother and sister for their love, guidance, understanding, encouragement and supports all of my life.

Financial supports was provided by Royal Golden Jubilee Ph.D. program (Grant No. PHD/0160/2553), and Chulalongkorn University.

## CONTENTS

	Page
THAI ABSTRACT .....	iv
ENGLISH ABSTRACT.....	v
ACKNOWLEDGEMENTS .....	vi
CONTENTS.....	vii
INTRODUCTION .....	9
Background and rationale .....	9
Research questions.....	11
Hypotheses.....	11
Objectives .....	11
Expected benefit .....	11
Conceptual Framework.....	12
REVIEW OF RELATED LITERATURE .....	14
Osteogenesis Imperfecta.....	14
Defective mechanisms/pathophysiology of osteogenesis imperfecta.....	14
- Type I collagen synthesis .....	16
- Osteoblast differentiation and functions.....	18
<i>MBTPS2</i> gene .....	18
Membrane-bound transcription factor protease, site 2 ( <i>MBTPS2</i> or <i>S2P</i> ) .....	18
Phenotypic heterogeneity of <i>MBTPS2</i> .....	19
Target proteins of <i>S2P</i> .....	22
- <i>Sterol regulatory element-binding protein (SREBP)</i> .....	22
- <i>Activating transcription factor 6 (ATF6)</i> .....	22
- <i>Cyclic AMP-responsive element-binding protein 3 subfamily (CREB3 subfamily)</i> .....	23
Induced pluripotent stem cells (iPSCs).....	24
MATERIALS AND METHODS.....	26
Part I: To confirm etiologic and pathogenic of mutations in <i>MBTPS2</i> .....	26
Part II: To find out pathomechanism of X-OI .....	30

	Page
RESULTS .....	39
<i>MBTPS2</i> mutations are causative for X-OI .....	39
Mutations in <i>MBTPS2</i> affect S2P's functions .....	40
iPSCs generation.....	43
iPSCs Characterization .....	43
iPSCs derived MSCs (iMSCs).....	52
iMSC derived osteoblasts .....	53
Gene expression during osteoblast differentiation .....	56
DISCUSSION.....	62
REFERENCES .....	66
VITA.....	75





# CHAPTER I

## INTRODUCTION

### Background and rationale

Osteogenesis imperfecta (OI) or brittle bone disease is a genetic disorder characterized by deformities of bones and multiple bone fractures, associated with macrocephaly, blue sclerae, hearing loss, dentinogenesis imperfecta, and short stature. OI is genetically heterogeneous. About 85% of OI have autosomal-dominant mutations in the type I collagen genes, *COL1A1* or *COL1A2*. More recently, at least 15 genes causing autosomal recessive forms of OI were reported. The products of these genes (*CRTAP*, *P3H1/LEPRE1*, *PIIB*, *FKBP10*, *PLOD2*, *SERPINH1*, *BMP1*, *SERPINF1*, *IFITM5*, *CREB3L1*, *SP7/OSTERIX*, *TMEM38B*, *WNT1*, *SEC24D* and *SPARC/OSTEONECTIN*) play a role in many pathways involving in type I collagen process or osteoblast differentiation and function (1-3). No cases of X-linked OI have been reported.

Our group collected a family with OI whose inheritance showing an X-linked recessive mode (X-linked osteogenesis imperfecta, X-OI). Interestingly, it is the first observation suggesting that a gene on X chromosome can cause OI. This leads to our study attempting to identify a new disease gene for OI, which may open a venue to discover a new pathway involving bone formation.

The X-OI family was studied to find the causative gene. Several techniques were used including CGH array to investigate the rearrangement of X-chromosome, linkage analysis to narrow down the linked region on the X-chromosome, and targeted re-sequencing by next generation sequencing (NGS) to identify the variants in the linked region. For these candidate genes with possible etiologic mutations, co-segregation analysis, prediction programs, and a search for the variants in controls were performed. We identified *membrane-bound transcription factor peptidase, site 2* (*MBTPS2*) as a probably causative gene for X-OI. It changes a nucleotide at position 1376 from A to G (c.1376A>G) leading to amino acid changing from asparagine to

serine at position 459 (p.N459S). The mutation lies on the transmembrane domain, an important region for enzymatic activity. A few year later, we collected the second family with X-OI from another group. They found the mutation in the same genes, the mutation changes nucleotide G to C (c.1515G>C). Amino acid was changed from leucine to phenylalanine at position 505 (p.L505F). The second family strongly supports the *MBTPS2* is a causative gene for OI. In my thesis, we did many studies to provide evidences that these two variants in the *MBTPS2* gene are actually pathogenic. We published them on *Nature Communications* in 2016 (4).

The second part of my thesis is to study deeper into the pathomechanism of how *MBTPS2* mutations could lead to OI phenotype using iPSC technology. *MBTPS2* encodes site 2 protease (S2P) that is an enzyme playing a role in regulated intramembrane proteolysis (RIP) (5). S2P's target proteins that have been identified can be separated in three groups, SREBP, ATF6, and CREB3 subfamily (6-8). There are several studies show involvement of those with osteoblast differentiation. SREBP is a well-known protein regulating cholesterol homeostasis. A few studies of it link to osteoblast differentiation. ATF6 and CREB3 subfamily involve in ER stress response and osteoblast differentiation. Mutations of *MBTPS2* have been reported to cause several dermatological genetic disorders, including Ichthyosis follicularis with atrichia and photophobia (IFAP) syndrome, keratosis follicularis spinulosa decalvans, X-linked (KFSDX), and Olmsted syndrome (9-12). Severe forms of these diseases are associated with lower levels of residual mutated protein activities.

S2P's target proteins show cell type-specific functions. For example, CREB3L1 plays a key role to response ER stress in astrocytes whereas it regulates *COL1A1* expression in osteoblasts. A cell type investigated in this study should represent pathology of the phenotype. With OI shows abnormalities in bones, the cell type using in the study should be osteoblasts. Osteoblasts can be derived from bone, bone marrow or connective tissues. At that time, we did not bone samples from our patient. Therefore, induced pluripotent stem cells (iPSCs) were chosen because it can be differentiated to any cell types. Fibroblast's patients were induced to iPSCs, then differentiate them to osteoblasts.

In this study, we present two independent X-OI pedigrees without symptoms of dermatological disorders. Two novel *MBTPS2* missense mutations were identified were

proved to be pathogenic. After *MBTPS2*, the latest causative gene for X-OI, has been identified, we investigated the mechanisms leading to X-OI caused by the *MBTPS2* p.N459S and p.L505F mutations in iPSC-derived osteoblasts.

### Research questions

1. Whether the identified p.N459S and p.L505F mutations in *MBTPS2* are pathogenic?
2. What are the pathomechanical pathways of the *MBTPS2* mutations leading to X-OI?

### Hypotheses

*MBTPS2* encodes S2P, a protease. It cleaves target proteins to active forms to act as transcription factors. The mutations affect the S2P's functions and result in decreasing active forms of target proteins, and in turn, lowering expression of their downstream genes involving in osteoblast differentiation. Different *MBTPS2* mutations may have various effects on each target protein leading to phenotypic heterogeneity. The inability to induce its downstream genes involving in osteoblast differentiation may lead to OI.

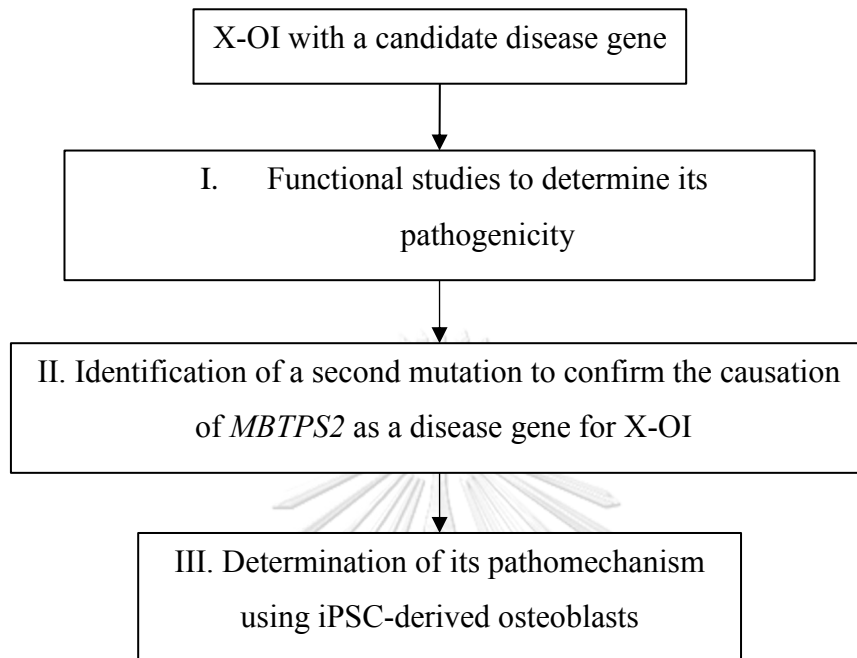
### Objectives

1. To demonstrate pathogenicity of the mutations, p.N459S and p.L505F, in the *MBTPS2* gene
2. To investigate pathomechanical pathways of the *MBTPS2* p.N459S and p.L505F mutations leading to X-OI.

### Expected benefit

This research may elucidate a pathway leading to X-OI. It may provide a better understanding of a normal bone formation, which may lead to new preventive and curative measures of bone diseases.

## Conceptual Framework



Three diagrams shows the detail in each study of conceptual framework: I, II and III

Diagram I.

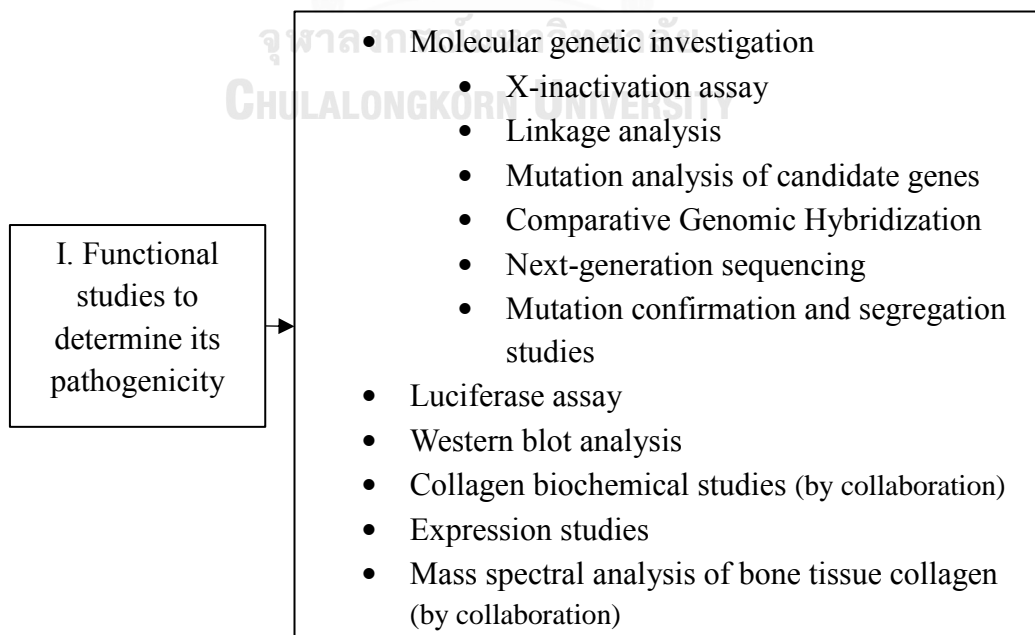


Diagram II.

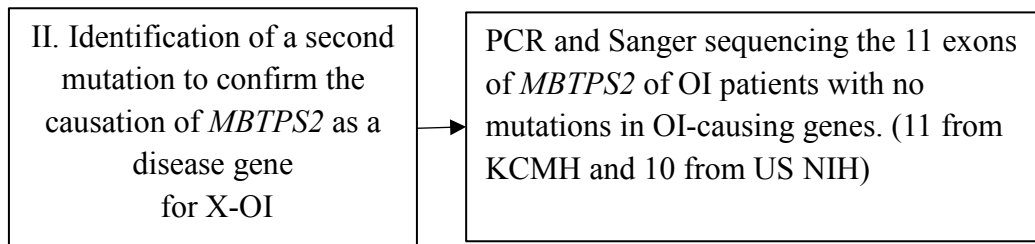
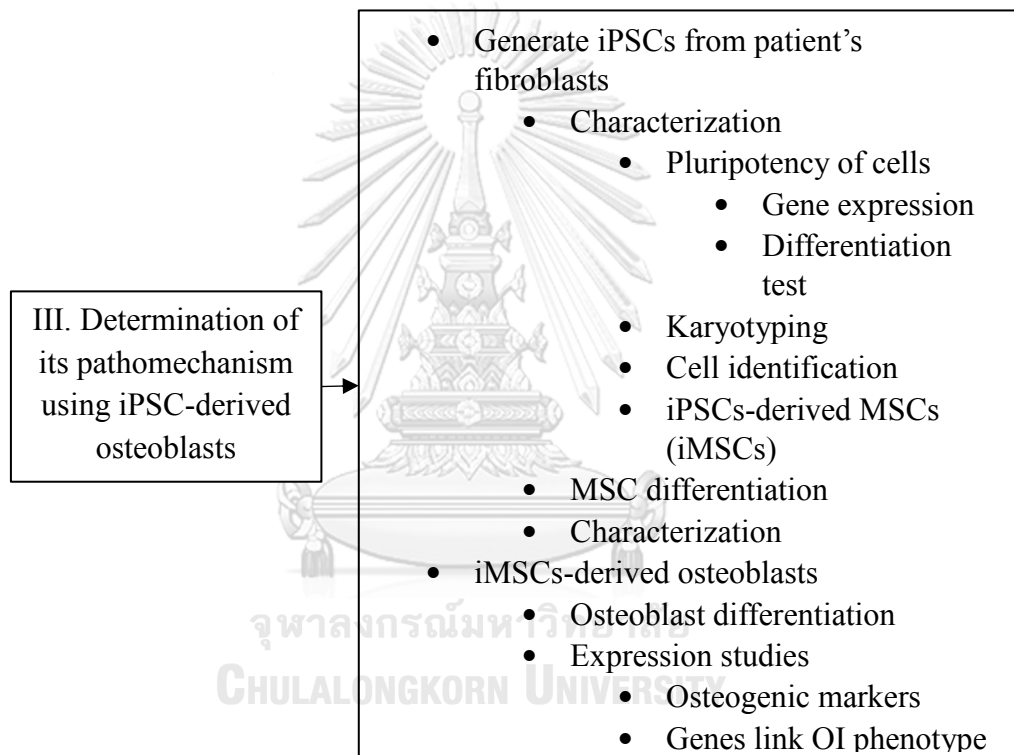


Diagram III.



## CHAPTER II

### REVIEW OF RELATED LITERATURE

#### Osteogenesis Imperfecta

Osteogenesis imperfecta (OI) or also known as brittle bone disease is a congenital disorder characterized by low bone mass, multiple bone fractures, growth deficiency associated with blue sclerae, hearing loss, dentinogenesis imperfecta and neurological defects (13). Clinical features show a wide range from mild to severe symptoms and neonatal lethality. In 1979, Sillence *et al.* classified OI to four groups, based on mode of inheritance, clinical presentation and radiographic features (Table 1) (13).

Table 1: Classification of osteogenesis imperfecta (modified from Sillence)

Type of OI	Characterization
Type I	blue sclerae, late-onset hearing loss, near-normal stature.
Type II	perinatally lethal form
Type III	progressive deforming variety
Type IV	similar to type I but more severity, short stature, bone deformity and dentinogenesis imperfecta

#### Defective mechanisms/pathophysiology of osteogenesis imperfecta

A decade after OI classification, only *COL1A1* and *COL1A2* were identified to be causative genes for OI (14). After that, a novel causative genes for OI were identified based on candidate gene approach, relating in type I collagen synthesis, or positional cloning approaches. Until the invention of a new technique, Next Generation Sequencing (NGS), several new causative genes for OI were discovered. *SERPINF1* is the first gene that identified by exome sequencing in 2011(15). Then, several genes that responsible for OI were identified by NGS such as *TMEM38B* (16), *IFITM5* (17),

*WNT1* (18), *SEC24D* (19), *SPARC* (20) including *MBTPS2* using combination of linkage analysis and targeted sequencing, a part of NGS (4).

Now, more than 18 genes have been reported to cause OI. These genes are tools to help researchers to further understand the mechanisms relating bone formation. The mutations in these genes show the defect mechanism leading to bone abnormalities. If we understand pathomechanism of those genes, we might know how to generate normal bone or treat the diseases with bone abnormalities. In this thesis, we divided the defective mechanisms of OI into two parts. The first part is involved in type I collagen synthesis and another part is osteoblast differentiation and functions. The causative genes were classified depending on defective mechanisms in Table 2.

Table 2. Overview of osteogenesis imperfecta based on causative genes and defective mechanisms

Defect mechanisms	Inheritances	Defective genes
Type I collagen synthesis		
- quantitative and structural procollagen	AD	<i>COL1A1 /COL1A2</i>
- collagen modification	AR	<i>CRTAP/LEPRE1/ PPIB</i>
- processing and crosslink	AR	<i>SERPINH1/FKBP10/ PLOD2/BMP1/ SEC24D</i>
Osteoblast differentiation and functions		
- osteoblast differentiation	AR	<i>SP7(OSTERIX)</i>
	AR/AD	<i>WNT1</i>
	AR	<i>CREB3L1</i>
	AR	<i>SPARC</i>
- bone mineralization	AD	<i>IFITM5</i>
	AR	<i>SERPINF1</i>

Abbreviations: AD, autosomal dominant; AR, autosomal recessive; XR, X-linked recessive.

## - Type I collagen synthesis

The most abundant component of the extracellular matrix in bone is type I collagen. It is produced from osteoblasts. *COL1A1* and *COL1A2* genes synthesize the pro  $\alpha 1(I)$  and pro  $\alpha 2(I)$  chains for assemble it to type I collagen in 2:1 ratio, respectively. Type I collagen comprises of N-terminal globular, helical domain and C-terminal globular. The helical domains contain the uninterrupted triplet repeats, Gly-Xaa-Yaa, because the glycine, a smallest amino acid, fits in the internal helical space. After translation, pro-alpha subunits were hydroxylated and glycosylated on the specific position by enzymes to modification for folding, transport and secretion. Then procollagen were cleaved to collagen and assembled to fibrillar collagen on extracellular matrix.

### o Quantitative and structural procollagen

More than 80% of OI patients have mutations in *COL1A1* and *COL1A2* genes (21). The mutations in these genes defect both of quantity and structure of type I collagen. Premature termination codon is the most quantitative defects, due to the nonsense-mediated mRNA decay. The decreased type I collagen causes mild OI phenotype, OI type I. Structural defects show severe form of OI, type II, III, or IV. It causes from glycine substitutions in helical domain resulting to abnormality of pro  $\alpha 1, 2(I)$  chains leading to abnormal structure of type I collagen (22-24).

### o Collagen modification

Post-translational modifications have multiple steps, mostly occurring in endoplasmic reticulum (ER). *CRTAP*, *LEPRE1* and *PPIB* were causative genes for OI in recessive inheritance encoding the components of prolyl 3-hydroxylation complex. It is responsible for 3-hydroxylation of prolyl residue at position 986 of pro  $\alpha 1(I)$  and 707 of pro  $\alpha 2(I)$  chains (25-27). Mutations in these genes lead to the excess of post-translational modification (28). Recent data showed lacking of prolyl 3-hydroxylation at 986 of pro  $\alpha 1(I)$  affects strength of fibrillar collagen (29). In addition to prolyl 3-hydroxylation, the complex prevent premature aggregation of type I collagen because the *PPIB* also acts as a chaperone (30).



- Collagen processing and crosslink

Collagen processing includes folding, quality control, transport, secretion and trimming of procollagen to collagen. Then, collagens are crosslinked by many enzymes such as lysyl hydroxylase and lysyl oxidase to assembly collagens to fibrillar collagens. In each process, several genes are involved. In this thesis, we focused on the causative genes for OI involving in these processes.

*SERPINH1* and *FKBP10* encode the chaperone-like proteins. Their functions monitor the correction and stability of newly formed triple helix of procollagen type I (31, 32). Heat shock protein 47 (HSP47) produces from *SERPINH1*. It is a collagen-specific chaperone. It has RDEL recognition site to transport proteins from ER to Golgi. (33). *FKBP65* encodes *FKBP10*, the largest member of the immunophilin subfamily, containing multiple ligands including type I collagen and PPIase domain (34). In addition to causing OI, it also causes of Bruck syndrome type I characterized by congenital contractures with pterygia, onset of fractures in infancy or early childhood, postnatal short stature, severe limb deformity, and progressive scoliosis(35).

*PLOD2* encodes lysyl hydroxylase 2 (LH2) being an enzyme to hydroxylation lysine at telopeptide of type I collagen to initiation crosslink within collagen fibrils. It leads to stability and tensile properties of collagen fibrils (36, 37). Like *FKBP10*, *PLOD2* causes of two diseases, OI and Bruck syndrome type II (38). Schwarze, *et al.* (2013) reported that these three genes, *SERPINH1*, *FKBP10* and *PLOD2* involve in procollagen maturation. Mutations in these genes affect bone mass and quality and lead to contracture (39).

*BMP1* encodes the metalloprotease bone morphogenic protein-1 (BMP1). It acts as a carboxy-(C)-proteinase to trimming carboxyl terminal of type I collagen to initiation of collagen fiber formation. If BMP1 is defective, the presence of carboxyl group on type I collagen affects structure of collagen fiber and leads to hypermineralization (40, 41).

*SEC24D* encodes a protein being a component of COPII complex. COPII complex exports several proteins including type I collagen from ER. Until now, there are only three reported that *SEC24D* causes of OI (19, 42, 43). The pathomechanism of *SEC24D* is still under investigations.

#### - **Osteoblast differentiation and functions**

Osteoblasts are bone producing cells. The origin of cells are mesenchymal stem cells (MSCs). There are multiple steps turning MSC to mature osteoblasts. Recently, some of the genes, *SP7*, *WNT1*, *CREB3L1* and *SPARC*, involving in the steps have been associated with OI (18, 20, 44, 45). However, the pathomechanism of these genes remain elusive.

Bone mineralization is a process to provide strength and flexibility to bones. Osteoblasts secrete calcium and phosphate. These are composed to hydroxyapatite (HA) and laid down in the ECM. This process is called mineralization. Its defects, either hypo- or hyper-mineralization cause abnormality of bones. Recently, there are two causing-genes for OI, *IFITM5* and *SERPINF1* associated with mineralized defects (15, 17, 46, 47).

#### ***MBTPS2* gene**

##### **Membrane-bound transcription factor protease, site 2 (MBTPS2 or S2P)**

*MBTPS2* is located on Xp22.12-p22.11 (12). It comprises eleven exons encoding 519 amino acids of a zinc metalloprotease. It encodes site-2 protease (S2P) comprising six transmembrane segments, TM1-TM6. It has two motifs that are conserved, the canonical metalloprotease motif (HEXXH) and NDPG motif (48, 49).

This protein, S2P, cooperates with site 1-protease (S1P). They play a role in regulated intramembrane proteolysis (RIP). S1P and S2P belong to intramembrane cleaving proteases (iCLiPs). There are three distinct iCLiPs families including the aspartyl protease-like, the zinc metalloproteinase site-2 protease, and the serine protease family of rhomboids. They locate in Golgi membrane. When their target proteins translocate to Golgi, S1P cleaves the first site and followed by S2P, which

cleaves the second. These target proteins include SREBP, ATF6 and CREB3 subfamilies (5).

### **Phenotypic heterogeneity of *MBTPS2***

*MBTPS2* was previously reported to cause of several dermatological diseases. These include ichthyosis follicularis, alopecia, and photophobia (IFAP) syndrome, keratosis follicularis spinulosa decalvans, X-linked (KFSDX), and Olmsted syndrome (9, 11, 12). IFAP is characterized by a triad of follicular ichthyosis, total or subtotal atrichia, and photophobia (12). KFSDX is characterized by development of hyperkeratotic follicular papules on the scalp followed by progressive alopecia of the scalp, eyelashes, and eyebrows. Associated eye findings include photophobia in childhood and corneal dystrophy (11). Olmsted syndrome is characterized by bilateral mutilating palmoplantar keratoderma and periorificial keratotic plaques (9). All of the dermatological diseases shared several features; however, the phenotype of X-OI, even though are caused by mutations in the same gene, differs from those of the aforementioned skin disorders significantly.

Several mutations have been found in *MBTPS2* (4, 9, 11, 12, 50-55) (Table 3 and Figure 1). Genotype-phenotype correlation of *MBTPS2* was reported in 2013 by Bornholdt, *et al.* The small levels of residual activity of S2P are associated with severe forms of the dermatological diseases (50). However, this research investigated only S2P's ability to cleave SREBP, one of many downstream target proteins of S2P.

Table 3. Reported mutations in *MBTPS2* with dermatological diseases and X-OI

<b>Disease</b>	<b>Mutation</b>	<b>Ref</b>
<b>IFAP</b>	M87I	12, 47
	W226L	12
	H227L	12
	F229S	47
	G253A	47
	C334Y	49
	R429H	12, 47, 51
	F475S	12, 47
	L476S	47
	D477V	47
	A478D	50
	L513P	47
	<b>KFSDX</b>	I258M
<b>IFAP/KFSDX</b>	G500D	47
	N508S	11, 47, 48, 52
<b>X-OI</b>	N459S	4
<b>Olmsted</b>	F464S	9

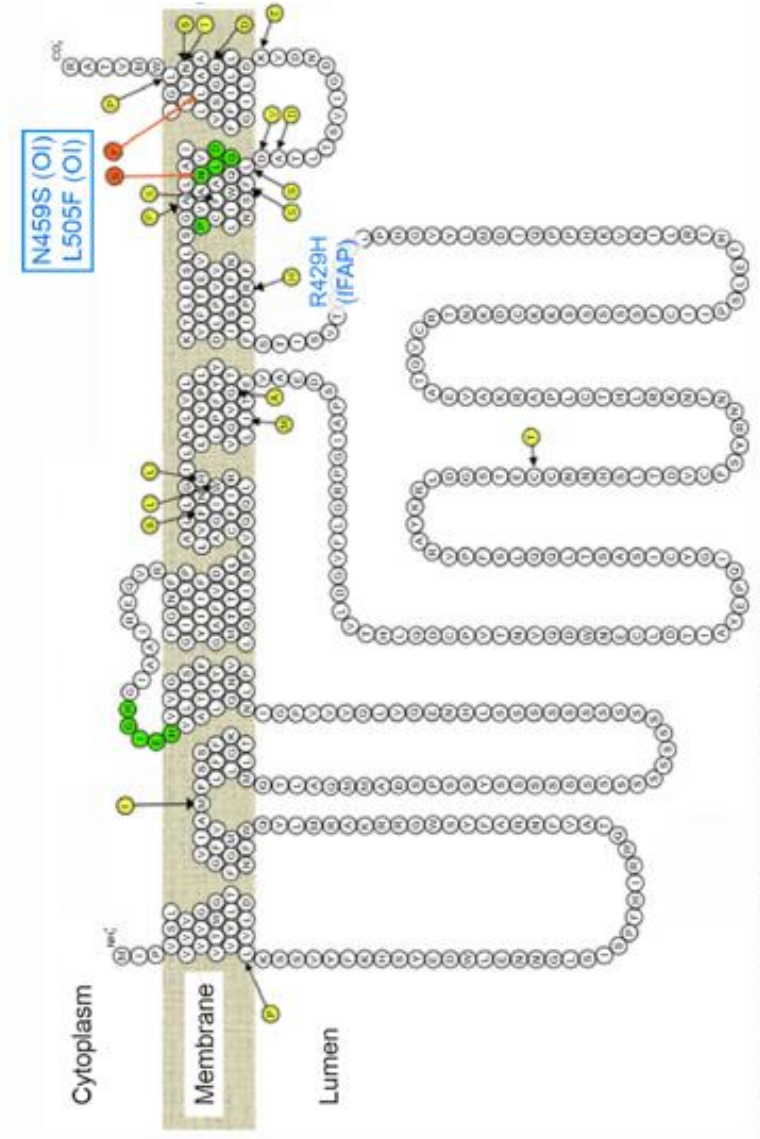


Figure 1. Map of *MBTPS2* mutations (4)

Green circle: represent the HEIGH and LDG/NPDG Motifs.

Yellow circle: represent *MBTPS2* substitutions in probands with IFAP, BRESHECK, KFSDX and Olmsted.

Red circle: represent *MBTPS2* substitutions in probands with X-OI.

Amino acid substitutions labeled in blue represent cell lines used for functional studies.

## Target proteins of S2P

Target proteins of S2P include SREBP, ATF6 and CREB3 subfamily. S2P cleaves these proteins and turns them into activated proteins involving in several mechanisms, such as cholesterol homeostasis (56), ER stress response (7), osteoblast differentiation (57, 58) and type I collagen synthesis (59). In this thesis, we focus on four S2P's target proteins, SREBP, ATF6, CREB3L1 and CREB3L3 owing to their functions relating to bone formation.

### - *Sterol regulatory element-binding protein (SREBP)*

Sterol regulatory element-binding proteins (SREBPs) are members of the basic helix-loop-helix-leucine zipper (bHLH-Zip) transcription factor family. In human, three members have been identified, SREBP1-a, SREBP1-C and SREBP-2 (60). These proteins have been shown to regulate genes involving in cholesterol synthesis and homeostasis (61, 62). When cells are starved of cholesterol, SREBPs would be translocated to Golgi and released active transcription factor by S1P and S2P (63). In addition to control cholesterol pathways, some reports found the relation between SREBP1 and mineralization (64-66).

### - *Activating transcription factor 6 (ATF6)*

*ATF6* encodes a type II transmembrane protein. It has four domains including transactivation domain (TAD), basic leucine zipper (bZIP), transmembrane domain, and luminal domain. The induction of ER stress to ATF6, embedded in ER membrane, liberates and translocates to Golgi. ATF6 is a transcription factor. Its downstream genes include a group of genes responding to ER stress such as *XBPI* (67). In addition, a recent report showed that ATF6 regulated genes involving in osteoblast differentiation (57, 58).

Both pathways, ER stress response and osteoblast differentiation, are possible mechanisms that cause the bone fragility in X-OI. In 2008, Lisse, *et al.* showed a new model for OI. They found that the abnormal type I collagen affected the ability of ER stress response leading to osteoblast apoptosis (68). In addition, there were reports which demonstrated the relationship between ATF6 and osteoblast differentiation.

Jang, *et al.* have proved that *Ocn*, which is a marker for mature osteoblasts, is a downstream gene of ATF6 (58). Tohmonda, *et al.* found that IRE $\alpha$ 1-XBP1 pathway regulated *Osx* transcription (57). *Osx* plays a key role in osteoblast differentiation by inhibiting Wnt signaling. This process turns pre-osteoblasts to mature osteoblasts (69). XBP1 is a downstream gene of ATF6 (67). Taken together, ATF6 might involve osteoblast differentiation by mediated two axis, ATF6-OCN and ATF6-XBP1-OSX.

In 2015, Kohl, *et al.* reported that homozygous mutations in *ATF6* cause the cone dysfunction disorder achromatopsia, characterized by a lack of cone photoreceptor function. A homozygous missense mutation, p.Arg324Cys, showed the defect of ATF6 transcriptional activity. Other mutations are frameshift and splice defects, and disperse through whole the *ATF6*. From the evidence, we hypothesize that ATF6 is not a major mechanism for pathogenesis of X-OI (70).

- *Cyclic AMP-responsive element-binding protein 3 subfamily (CREB3 subfamily)*

The CREB3 subfamily has five members including CREB3, and CREB3L1-L4. They are type II membrane-associated proteins. The N-terminus lies in the cytoplasm whereas the C-terminus penetrates through the ER membrane (71, 72). Similar to ATF6, they are transcription factors and S2P's target proteins. Cell type-specific functions were shown in these proteins. In osteoblasts, CREB3L1 and CREB3L3 show the evidences involving in bone formation (73). CREB3L1 involves in type I collagen synthesis which is an important protein in bone formation (59). CREB3L3 has been reported that it rescued mineralization in defective S1P-cells (64).

- *cAMP response element-binding protein 3-like 1 (CREB3L1)*

Structure of *CREB3L1* or *OASIS* is similar to that of *ATF6*. It also has four domains, resides at the ER membrane and is stimulated by ER stress (6). However, the downstream genes of CREB3L1 are different from ATF6. CREB3L1 is a cell type-specific transcription factor. In each cell types, its downstream genes are different. In astrocytes (74), its targets are a group of ER stress response. In osteoblasts (59), its targets are a group of collagen synthesis, while in pancreatic beta-cells (75), its targets are a group of

proteins in secretion pathway. In animal model study, *CREB3L1*<sup>-/-</sup> knockout mice showed severe osteopenia that involves to type I collagen decreasing. It also found decreasing of *COL1A1*, downstream gene of CREB3L1, only in bone but not found in skin fibroblasts. (59). In 2013, there is a report that show homozygous deletion of *CREB3L1* associated with severe OI in human. Like *CREB3L1*<sup>-/-</sup> knockout mice, biochemical procollagen in patient's skin fibroblasts did not show obvious abnormalities, in both of quality and quantity. These reports support the involvement of *CREB3L1* to bone formation and tissue-specific functions (44).

○ *cAMP response element-binding protein 3-like 3 (CREB3L3)*

CREB3L3 or CREB-H was firstly reported to be a liver-specific transcription factor (76). After that, there are several studies to identify its functions. It shows several functions including innate immunity (77), gluconeogenesis (78), and lipid metabolism (79).

Some reports showed involvement of CREB3L3 in osteoblasts. The first report, investigation in osteosarcoma cell line with deficient of S1P found that overexpression of active form of CREB3L3 can rescue mineralization. In addition, microarray analysis in HEK-293 revealed that overexpress active form of CREB3L3 upregulated several genes including SEC24D, SPARC, and LOX. The first two genes are causative genes for OI, while the last plays a key role in collagen assembly (80). Recently, Jang, W. *et al*, reported that overexpression of CREB3L3 suppressed osteogenic markers, RUNX2, ALPL, OCN, in primary osteoblasts (81).

### **Induced pluripotent stem cells (iPSCs)**

In 2006, a new technology to change mouse somatic cells to cells maintaining the properties like embryonic stem cells (ESCs) was discovered by Yamanaka, *et al*. It used four transcription factors, OCT4, SOX2, KLF4 and c-MYC, called Yamanaka factors. The cells were generated to ESCs-like cells calling induced pluripotent stem cells (iPSCs) (82). After one year, other research groups were able to generate human iPSCs (83, 84).



iPSCs still have pluripotency and self-renewal capacities like ESCs. They proliferate indefinitely *in vitro* and can be differentiated into all cell types. With these properties, researchers use them as ‘human disease in a dish’. They investigate pathomechanism and drug screening on them and use human iPSC products to treatment, so call cell-based therapy (85).

Like monogenic disorders, OI-iPSCs were used to study mechanisms of novel causative genes and also generated iPSCs products to treatment. In 2012, Daley, *et al.* generated iPSCs from MSCs of OI patients that inactivated their mutant collagen genes by adeno-associated virus (AAV)-mediated gene targeting. They found that gene-targeted iPSCs-derived MSCs produced normal collagen. The combination of gene targeting and iPSC derivation can be used to produce potentially therapeutic cells (86). In 2016, Belinsky, *et al.* generated iPSCs from peripheral leukocytes of OI patient with null mutation in *PEDF* to investigate PEDF’s role in osteoblasts. They found abnormalities in secreted matrix proteins which were normalized by exogenous PEDF (87).

There are four factors to be considered in iPSCs generations including the donor cell type, the reprogramming cocktails, the culture condition and the delivery system. The donor cell type was concerned in aspects of cell availability, efficiency and kinetics of reprogramming. Peripheral leukocytes and fibroblasts are frequently used to be a donor cell type because they are easy to collect and have high efficiency to reprogram. The reprogramming cocktails were selected depending on pluripotency, cell proliferation and epigenetic of donor cell type. For the culture condition, parameters include the feeder cells and medium composition. The suitable culture condition will support cells undergo reprogramming. The delivery system, in present, is to transport the reprogramming cocktails to cells. These are classified into two systems, integrative and non-integrative approaches, depending on the genetic materials whether they can be integrated to host genome (88).

In this thesis, we used fibroblasts from X-OI patients to generate iPSCs by using Yamanaka factors. In culture conditions, we used human foreskin fibroblasts to feeder cells and ESC medium to medium composition. Concerning the last factor, Sendai virus and episomal vector, the non-integrative delivery systems, were used.

## CHAPTER III

### MATERIALS AND METHODS

#### **Part I: To confirm etiologic and pathogenic of mutations in *MBTPS2***

To validate causation of the mutation, p.N459S, in the *MBTPS2*. We find the unrelated second family with OI who maintain the mutation in *MBTPS2* using direct sequencing all exons. 21 OI patients from King Chulalongkorn memorial hospital (KMCH) and 40 patients from our collaboration, National Institute of Child Health and Human Development, USA were direct sequenced. 10 patients from KMCH and 30 patients from NIH-USA did by Ausavarat S.

To demonstrate pathogenicity of the mutations, p.N459S and p.L505F, in the *MBTPS2*. We investigated the stability of RNA and protein of S2P and tested the cleavage activity of it on its target proteins, ATF6, SREBP and CREB3L1. Part of SREBP did by Ausavarat S.

Stability of RNA and protein of S2P were study using real-time RT-PCR and western blot analysis. The transcription activity of ATF6 and SREBP was investigated by using luciferase assay. Level of luciferase expression indirectly represents the level of active forms of ATF6 and SREBP reflecting to cleavage activity of S2P. To confirm the result from luciferase assay, we investigated protein level of HSPA5, downstream gene of ATF6, using western blot analysis. CREB3L1 was observed size of cleaved protein by western blot analysis, due to the cleaved form by S1P and S2P, 55 and 50 kDa respectively, can be detected. It is direct evidence to show S2P's cleavage activity.

Real-time RT-PCR: To investigate RNA stabilities of each mutation in *MBTPS2*

1. RNA was extracted from primary fibroblasts of the patients using QIAamp RNA blood mini kit (Qiagen).
2. Quantitate RNA with NanoDrop (Thermo Scientific).

3. Reverse RNA to Complementary DNA with ImProm-II Reverse Transcription System (Promega).
4. Taqman Gene Expression Assays were used to determine the transcript level of *MBTPS2* (Hs00210639\_m1) and *GAPDH* (Hs02758991\_g1), that is internal control)

Luciferase assay: To investigate S2P's cleavage activities on ATF6

1. Culture CHO-M19, S2P deficient cell line, in Ham's F-12 medium supplement with 10% fetal bovine serum (Sigma) and 1X penicillin/streptomycin (Hyclone) at 37<sup>o</sup> C with 5% CO<sub>2</sub> at density of 1.5X10<sup>5</sup> cell/well in triplicate in 12-well plate.
2. After 24 hours, cells were transiently transfected with 800 ng of p5XATF6-GL3, 1 mg of expression plasmid containing wild type, mutant (R429H, N459S, L505F) of *MBTPS2* and no insert and 50 ng of pRL-SV40 as a transfection control. pdEYFP-C1amp were used to adjusted total amount of DNA to 2 mg/well. TurboFect (Thermo Scientific) were used for the transfection.
3. After 24 hours, add 2 mg/ml of tunicamycin/DMSO in cells to stress induction. Untreated cells were added 0.2% DMSO.
4. After 24 hours, the firefly and renilla luciferase activities were measure using a dual luciferase assay system (Promega).

List of plasmids were used in the experiment

- Reporter plasmids
  - p5XATF6-GL3: firefly luciferase expression with promoter containing ATF6 binding element
  - pRL-SV40: renilla luciferase expression
- Expression plasmids
  - pdEYFP-C1amp: expression plasmid
  - pdEYFP-MBTPS2: expression plasmid with wild type of *MBTPS2*

- pdEYFP-MBTPS2-R429H: expression plasmid contains *MBTPS2* with mutation at amino acid 429 changing arginine to histidine, it represents IFAP
- pdEYFP-MBTPS2-N459S: expression plasmid contains *MBTPS2* with mutation at amino acid 459 changing asparagine to serine, it represents X-OI patient
- pdEYFP-MBTPS2-L505F: expression plasmid contains *MBTPS2* with mutation at amino acid 505 changing leucine to phenylalanine, it represents X-OI patient

All mutations were created by QuikChange Site-Directed Mutagenesis Kit (Stratagene). All primers for created mutation were shown in Table 4.

Table 4. Mutagenesis primers

Primer	5'-3' sequences
pdEYFP-MBTPS2-R429H	Forward: GTGAGCATCACCAGTTTTATCCCACATTT TAACTTTCTAAGC Reverse: GCTTAGAAAGTTAAAATGTGGGATAAAA CTGGTGATGCTCAC
pdEYFP-MBTPS2-N459S	Forward: GAGCTCTGGCTATTGTTAGTGCAGTACC CTGC Reverse: GCAGGGTACTGCACTAACAATAGCCAGA GCTC
pdEYFP-MBTPS2-L505F	Forward: GTGGCAGTGTACTTTTCGCTGCCAATGT GACCC Reverse: GGGTCACATTGGCAGCGAAAAGTACACT GCCAC

### Western blot analysis

- To investigate protein stabilities of each mutation in MBTPS2
  1. Proteins were extracted from cell lysates from primary fibroblasts and collected in RIPA buffer supplemented with a protease inhibitor cocktail
  2. Measurement protein using Micro BCA Protein Assay Kit (Thermo scientific)
  3. Protein lysate (50 mg) was loaded per lane on a 12% SDS-PAGE
  4. Transfer protein to PVDF membrane using iBlot Dry Blotting System (Thermo scientific)
  5. Blocked with 5% BSA before probing with MBTPS2 antibody (Cell Signaling, #2157) overnight.
  6. Blots were washed, incubated with secondary antibodies for 1 hour.
  7. Detection protein with SuperSignal West Pico Chemiluminescent Substrate (Thermo scientific) and visualized on ImageQuant LAS 4000 (GE Healthcare Life Sciences).
  
- To investigate downstream gene of ATF6, *HSPA5*, and S2P's cleavage activity on CREB3L1

Primary fibroblasts of IFAP, two X-OI and CHO-M19 containing wild type and mutant constructs were grown to confluence and treated with tunicamycin (2 mg/ml) and/or ALLN (25 mg/ml) for 2 h before harvest. Tunicamycin induce ER stress resulting to release ATF6 and CREB3L1 to the location of S2P. ALLN protects the degradation of cleaved form of them. Protein detection followed by topic "To investigate protein stabilities of each mutation in S2P", except primary antibody changing from MBTPS2 to HSPA5 (Cell Signaling, C50B12) and CREB3L1 (R&D Systems, AF4080)

## Part II: To find out pathomechanism of X-OI

To investigate pathomechanical pathways of the *MBTPS2* p.N459S and p.L505F mutations leading to X-OI.

With OI shows abnormalities in bones, we used osteoblasts that is cell-producing bones for study. Osteoblasts in this thesis were generated from X-OI patients' fibroblasts using iPSC technology. When we got the iPSCs, they were characterized and differentiated to MSCs. Like iPSCs, MSCs were characterized and differentiated to osteoblasts. During differentiate MSC to osteoblasts, we collected RNA on day 0, 7, 10, 14 and 21 to investigate gene expression patterns in two aspects, osteogenic markers and pathomechanism. The end of osteoblast differentiation, calcium deposits were observed.

### Fibroblast isolation

1. Punch biopsy was obtained from X-OI patient's skin.
2. Collect skin biopsy in DMEM medium supplement with 3X penicillin/streptomycin (Hyclone)
3. Skin biopsies were cut to small pieces and placed on a culture plate, orientating the tissue so that the dermis is in contact with the bottom of the dish.
4. Incubate the plate 15 min at room temperature to allow good adhesion of the dermis onto the culture dish.
5. Gently add a small amount of medium (DMEM supplement with 20% fetal bovine serum and 1X penicillin/streptomycin) on the side of the biopsies.
6. Culture 48-72 hours in the 5% CO<sub>2</sub> incubator at 37°C. Fibroblasts were grown out of the biopsies.
7. Primary fibroblasts maintain in DMEM supplement with 10% fetal bovine serum, 1X penicillin/streptomycin and 4ng/ml basic-FGF.

## iPSCs Generation

Both Sendai virus and episome techniques are non-integrative system. In thesis, we used human foreskin fibroblasts (HFFs) are feeder cells and ESC medium for maintain iPSCs generating from these techniques. In episome technique, we used 4D-nucleofector (Lonza) for transport episomal vector into cells.

### - Sendai virus

We use CytoTune-iPS 2.0 Sendai Reprogramming Kit (Invitrogen) to reprogram patient's fibroblasts of IFAP containing R429H and X-OI containing N459S. Workflow for Sendai virus reprogramming shows in figure 2.

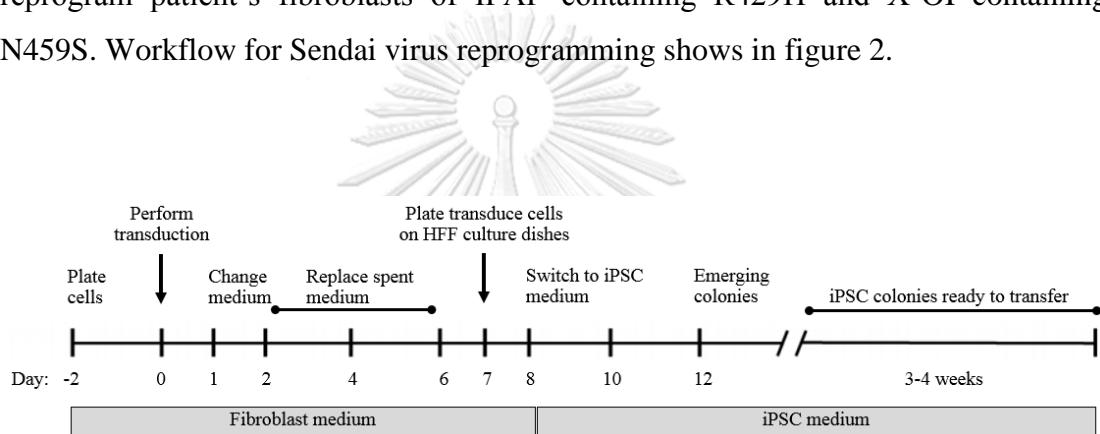


Figure 2. Workflow for CytoTune-iPS 2.0 Sendai Reprogramming Kit (Invitrogen)

### - Episomal vector

We use episomal vector from KIRA protocol (89-91) to reprogram patient's fibroblasts of X-OI containing L505F. Workflow for episomal reprogramming shows in figure 3.

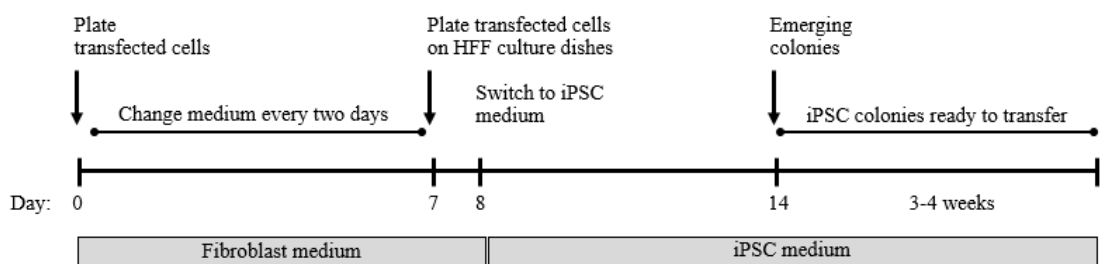


Figure 3. Workflow for episome (modified from KIRA protocol)

#### Feeder cells preparation

1. When HFFs confluent, cells will maintain in fibroblast medium supplement with mitomycin-C (sigma) in the 5% CO<sub>2</sub> incubator at 37°C for 2 hour.
2. Remove medium and wash the cells five times with 1X PBS (Hyclone)
3. Dissociate cell with 0.05% trypsin and incubate until the cells come off the plate (3-5 min.).
4. Add fibroblast medium and pipetting up and down to break up cell aggregation.
5. Count cells and plate cells at density 5X10<sup>5</sup> cells on 35mm culture dishes.
6. Incubate overnight and use cells as feeder layers in the next day and up to day seven. Change medium every other day.

#### iPSCs Characterization (92)

##### - ESC marker expression

To confirm their pluripotency by immunostaining. The antibody combinations we use include nuclear, OCT4 and NANOG, and surface markers, SSEA-4 and TRA-1-60.

1. Dissociate cells to a new culture dish that coated with Matrigel matrix (Corning) overnight.
2. Incubate in the 5% CO<sub>2</sub> incubator at 37°C until to iPSCs form packed colonies about 3-4 days.
3. Immunocytochemistry was used to detect those markers.
4. Primary antibody and secondary antibody show in Table 5.

##### - Differentiation test

To confirm iPSCs can differentiate to form tissues derived from the three primordial germ layers, endoderm, mesoderm and ectoderm, of the embryo. Antibodies for alpha fetoprotein (AFP), brachyury and nestin were used to represent in each germ layers.

1. Dissociate cells and plate on non-coated culture dish to cells perform embryoid bodies (EBs).



2. Maintain cells in ESC medium and EB medium in ratio 1:1 and incubate in the 5% CO<sub>2</sub> incubator at 37°C for 7 days. Change medium every other day.
  3. After 7 days, plate EBs on 3 Matrigel-coated culture dishes.
  4. Maintain cells in EB medium and incubate in the 5% CO<sub>2</sub> incubator at 37°C for 14 days. Change medium every other day.
  5. Immunocytochemistry was used to detect those markers.
  6. Primary antibody and secondary antibody show in Table 5.
- Immunocytochemistry (ICC)
1. Wash cells with 1XPBS.
  2. Fix cells with 4% paraformaldehyde.
    - a. ESC markers incubate for 15 minutes at room temperature
    - b. Differentiation test incubates for 20 minutes at room temperature
  3. Wash cells with 1X PBS at 3 times for 5 minutes.
  4. For nuclear markers, permeable cell membrane with 0.2% triton X-100 for 10 minutes at room temperature.
  5. Repeat step 3.
  6. Block cells with 5% fetal bovine serum for 1 hour at room temperature.
  7. Prepare primary and secondary antibody in 0.5% fetal bovine serum in 1:200 and 1:500, respectively.
  8. Add primary antibody from step 7 and incubate overnight at 4°C.
  9. Repeat step 3.
  10. Add secondary antibody from step 7 and incubate 1 hour at room temperature.
  11. Repeat step 3.
  12. Add DAPI and detect markers by fluorescence microscope.

Table 5. Antibodies for iPSCs characterization

Primary antibody	Secondary antibody	Marker detection
OCT4	Anti-Rabbit IgG	Nuclear pluripotent
NANOG	Anti-Rabbit IgG	Nuclear pluripotent
SSEA-4	Anti-Mouse IgG	Surface pluripotent
TRA-1-60	Anti-Mouse IgM	Surface pluripotent
AFP	Anti-Mouse IgG	Endoderm layer
Brachyury	Anti-Rabbit IgG	Mesoderm layer
Nestin	Anti-Mouse IgG	Ectoderm layer

- Cell identification

Generally, DNA finger print were used to identify iPSCs. For our iPSCs, each of cell line maintain specific mutation, so we used direct sequencing to identify our iPSCs.

- Karyotyping analysis

To evaluate genome integrity, traditional karyotype analysis were used. Cell were observed at metaphase stage by quinacrine staining under a microscope. Twenty metaphases were analyzed.

1. Add colchicine to cell at log phase and incubate in the 5% CO<sub>2</sub> incubator at 37°C for 3 hours.
2. Dissociate cells with 0.05% trypsin by standard protocol.
3. Wash cell with 1XPBS and collect cell pellet by centrifugation at 1200 rpm for 5 minutes.
4. Add 0.075M KCl and incubate in 37°C for 10 minutes and collect cell pellet by centrifugation.
5. Fix cell with methanol and acetic acid in 3:1 ratio and collect cell pellet. Repeat this step 3 times, except second time change ratio to 2:1.
6. Drop cell pellet to slide and observe metaphase cells under microscope.
7. Slides maintaining metaphase cells were stained with quinacrine and analyzed.

### iPSC-derived MSC (iMSC)

- MSC Differentiation protocol (modified from Hynes, *et al.* (93))
  1. Dissociate iPSCs with Versene (Invitrogen) to small clumps
  2. Plate cells on 0.1% gelatin-coated culture dishes.
  3. Maintain cells in MSC differentiation medium (IMDM supplement with 10% fetal bovine serum (Hyclone), 1X penicillin/streptomycin and 1X Glutamax (Invitrogen)) for 10-14 days. Morphology of cells at the edge of colonies were changed from epithelium to mesenchyme.
  4. Dissociate cells with 0.05% trypsin.
  5. Plate cells on 0.1% gelatin-coated culture dishes, cells are passage 1 (P1).
  6. After that, dissociate cells in 1:3 ratio in each passage.
  7. After passage 3, plate cells on standard culture dishes (non-gelatin-coated culture dish)
  8. Around P3-P4, cells are homogenous. Media are changed to MSC culture medium (alpha-MEM supplement with 10% fetal bovine serum, 1X Glutamax, 1X penicillin/streptomycin and 4 ng/ml basic-FGF).
  9. MSC markers are assessed by flow cytometry.

Workflow of MSC differentiation shows in Figure 4.

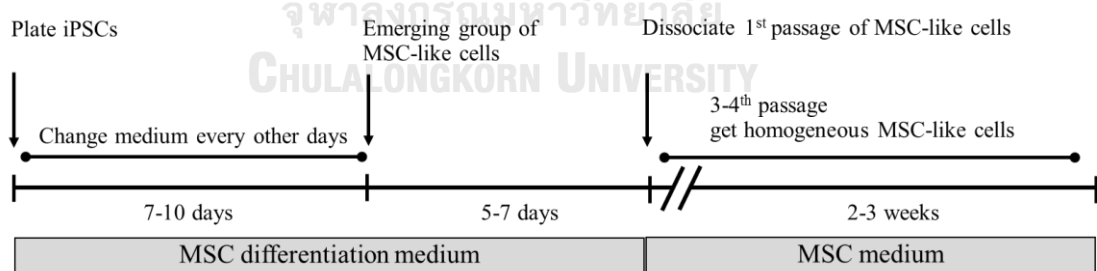


Figure 4. Workflow for MSC differentiation

### - MSC Characterization

To confirm cells that derived from iPSCs are MSCs, we investigate MSC properties including morphology, attachable to plastic, express MSC markers.

- o Morphology: observe cell morphology under microscopic

- Plastic attachable: culture cell on non-coated culture dish (after P3, cell culture on non-coated culture dish)
- MSC markers
  - CD44, CD73, CD90 and CD105 were assessed to identify MSCs by flow cytometry.
    1. Collect cells by trypsinization.
    2. Wash cells with 1X PBS for two times.
    3. Counting cells, and re-suspend cell in 0.1 ml 1X PBS at  $1 \times 10^5$  cells
    4. Add the conjugated antibody and incubate at room temperature in the dark for 15 minutes.
    5. Repeat step 2 and re-suspend cell in 0.1 ml 1X PBS for flow cytometry analysis

#### iMSC derived osteoblast

- Osteoblast differentiation (94)
  1. Dissociate MSCs by trypsinization
  2. Counting cell, and plate cells on 35 mm gelatin-coated culture dish at density  $5 \times 10^3$  cell/cm<sup>2</sup>
  3. Maintain cells in MSC culture medium for 2-3 days until cell grow up more than 80% confluency.
  4. Change media to osteogenic induction medium (DMEM supplement with 10% fetal bovine serum (Hyclone), 1X penicillin/streptomycin, 0.05 mM ascorbic acid, 10mM beta-glycerophosphate and 100nM dexamethasone) incubate 3 weeks. Change the medium every third day.
- Pathomechanism study
  - Expression study : osteogenic markers and genes link OI phenotype
 

We detect osteogenic markers, *ALP*, *RUNX2*, *COL1A1*, *SPP1*, *BGLAP* and genes involving in S2P's target proteins using real-time RT-PCR at day 0, 7, 10, 14, 21. *GAPDH* is used to internal control. (ATF6: *BGLAP*, *SP7*; CREB3L1: *COL1A1*; CREB3L3: *SEC24D*, *SPARC*, *LOX*)

Real-time RT-PCR

1. RNA was extracted from primary fibroblasts of the patients using QIAamp RNA blood mini kit (Qiagen).
2. Quantitate RNA with NanoDrop (Thermo Scientific).
3. Reverse RNA to Complementary DNA with ImProm-II Reverse Transcription System (Promega).
4. Taqman Gene Expression Assays were used to determine the transcript level of those of gene show in Table 6.

Table 6. Gene list for expression studies in osteoblast differentiation.

Gene	Taqman gene expression assay
Alkaline phosphatase ( <i>ALP</i> )	Hs1029144_m1
Bone gamma-carboxyglutamate protein/Osteocalcin ( <i>BGLAP/OCN</i> )	Hs01587814_g1
Collagen type I alpha 1 ( <i>COL1A1</i> )	Hs00164004_m1
Glyceraldehyde-3-phosphate dehydrogenase ( <i>GAPDH</i> )	Hs02758991_g1
Lysyl oxidase ( <i>LOX</i> )	Hs00942480_m1
Runt related transcription factor 2/ Core-Binding Factor Subunit Alpha-1 ( <i>RUNX2/CBFA1</i> )	Hs00231692_m1
SEC24 Homolog D, COPII Coat Complex Component ( <i>SEC24D</i> )	Hs00207926_m1
Secreted Phosphoprotein 1/Osteopontin ( <i>SPP1/OPN</i> )	Hs00959010_m1
Secreted Protein Acidic And Cysteine Rich/Osteonectin ( <i>SPARC/ON</i> )	Hs00234160_m1
Sp7 transcription factor/Osterix ( <i>SP7/OSX</i> )	HS01866874_s1

○ Calcium deposit

We used Alizarin RedS (ARS) (Sigma) staining to evaluate calcium deposit in qualitative and quantitative manners (95).

- Preparing 40 mM ARS, pH 4.1-4.3
  1. Dissolved 0.7 g ARS in 25 mL dH<sub>2</sub>O.
  2. Adjust pH to 4.1-4.3 with 0.5% ammonium hydroxide.
  3. Adjust final volume of ARS to 50 mL
- Qualitative calcium deposit by ARS
  1. Wash cells with 1X PBS
  2. Fix cells with 4% PFA at room temperature for 15 minutes
  3. Wash cells with distilled water at room temperature for 5 minutes in three times
  4. Add 40mM Alizarin red (pH 4.1-4.3) and incubate at room temperature for 30 minutes.
  5. Repeat step 3.
  6. Take pictures to document your findings.
- Quantitative calcium deposit by ARS
  1. After take pictures, add 10% acetic acid and incubate for 30 minutes with shaking.
  2. Collect cells by cell scraper to 1.5 mL microcentrifuge tubes.
  3. Vortex vigorously for 30 seconds.
  4. Heat at 85°C for 10 minutes
  5. Transfer tube to ice for 5 minutes.
  6. Centrifuge at 15,000g for 20 minutes.
  7. Collect supernatant to a new 1.5 mL microcentrifuge tube.
  8. Adjust pH to 4.1-4.3 with 10% Ammonium hydroxide.
  9. Measurement at OD405 with SpectraMax (Molecular devices)
  10. Analyzed data by comparing to standard curve of ARS

## CHAPTER IV

### RESULTS

#### ***MBTPS2* mutations are causative for X-OI**

We directly sequenced all of the exons of *MBTPS2* in 61 patients of OI from KMCH and US NIH. No obviously mutation was found in the gene. Few years later, US NIH got the second family who containing the mutation, p.L505F, in *MBTPS2* from a collaborator in Switzerland. The second family strongly supports that *MBTPS2* gene is a causative gene for X-OI. The patient's pedigree and clinical features of probands and mutation identification are shown in Figures 5 and 6.

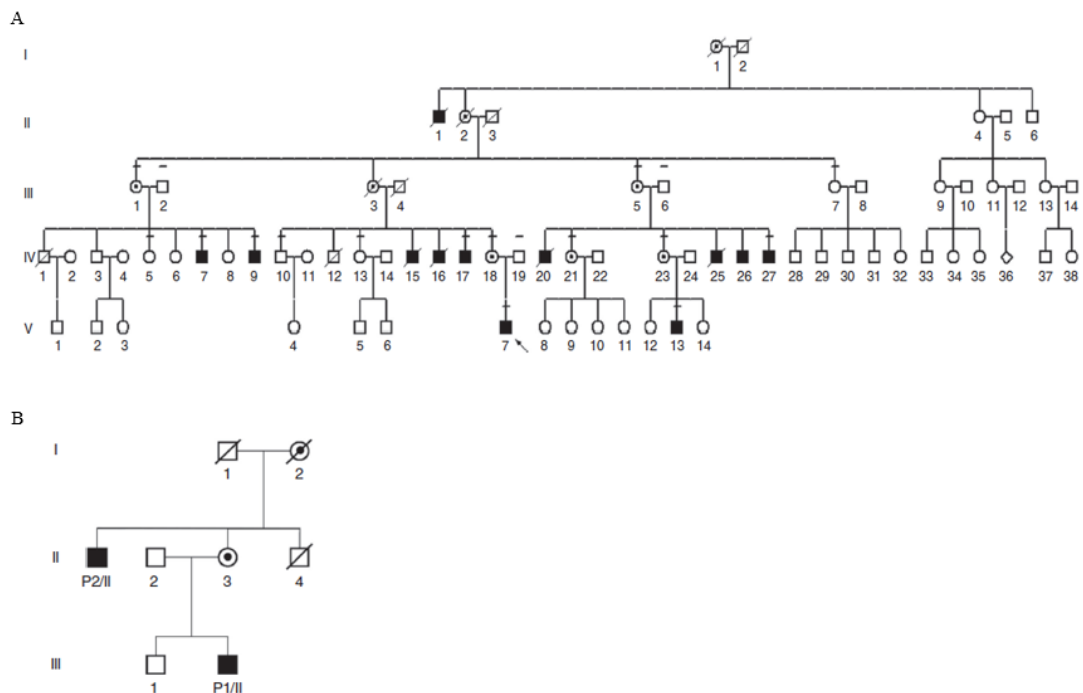


Figure 5. The patient's pedigrees with X-linked osteogenesis imperfect (A: pedigree of first family, B: pedigree of second family) (4)

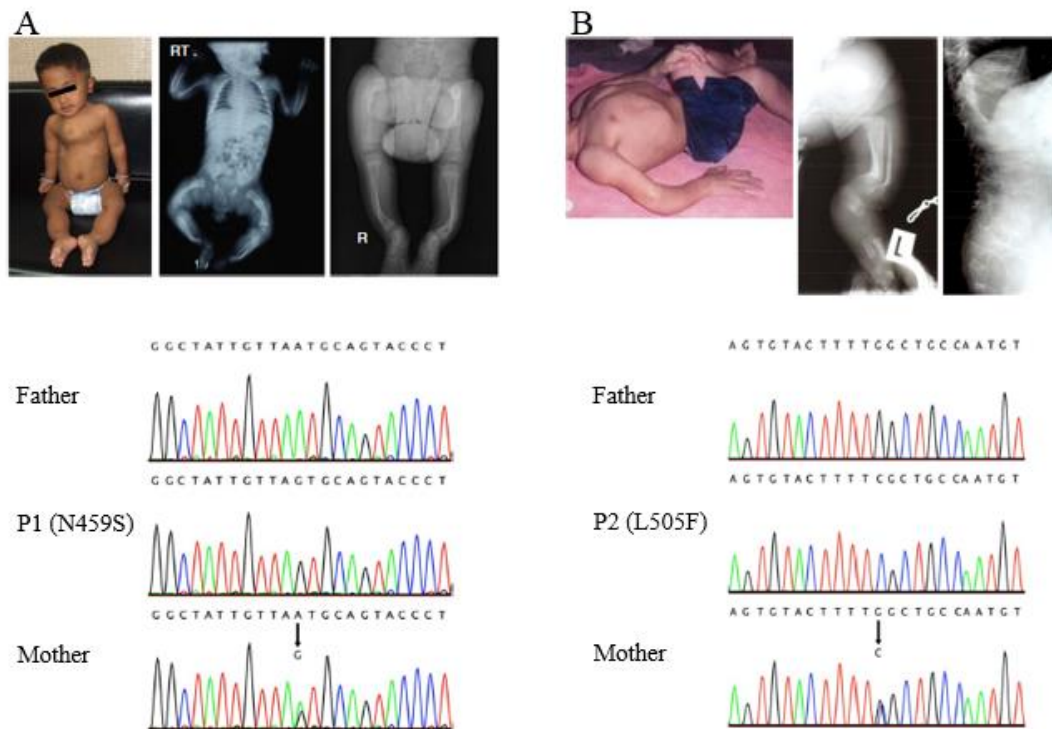


Figure 6. Clinical features of probands and mutation identification (A: first family, B: second family) (4)

### Mutations in *MBTPS2* affect S2P's functions

- Stability of RNA and protein of *MBTPS2*

Transcriptional levels of *MBTPS2* were not reduced in fibroblast with X-OI (N459S and L505F) and IFAP (R429H) mutations, by real-time RT-PCR (Figure 7A). S2P protein showed normal level in these cells (Figure 7B)



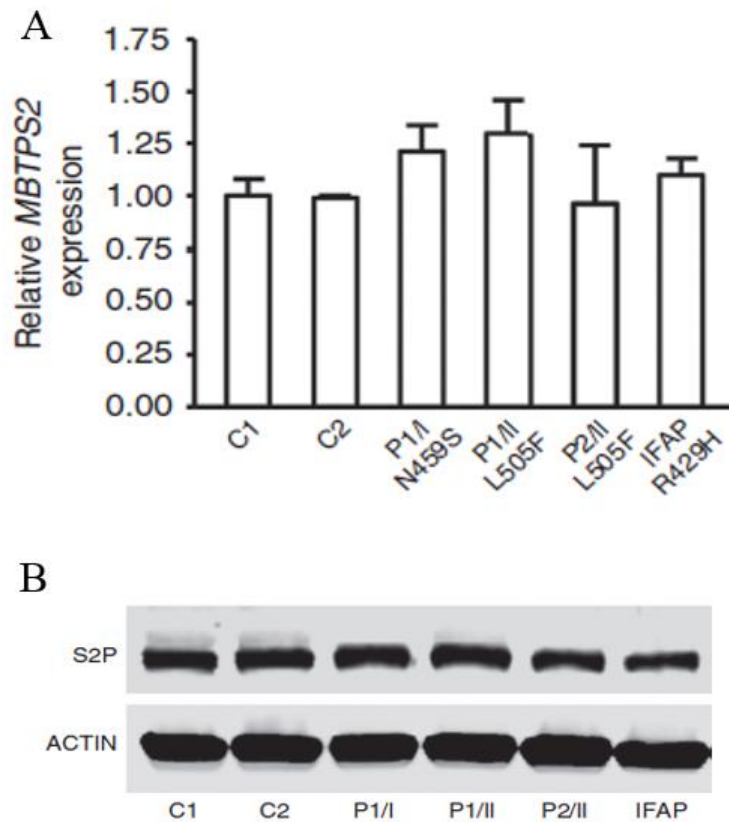


Figure 7. Expression of MBTPS2 in X-OI and IFAP fibroblasts. (A: gene expression, B: protein expression) (4)

- S2P's cleavage activities

o ATF6

We investigated the effect of S2P mutations on transcriptional activity of ATF6. CHO-M19, S2P deficient cells, that were transfected with mutant constructs (p.N459S, p.L505F, p.R429H) showed the decreasing of ATF6 activity in group of tunicamycin-induced ER stress versus normal *MBTPS2*, as measured by luciferase activity (Figure 8A). Furthermore, activation of the folding chaperone BiP, downstream gene of ATF6, was decreased in tunicamycin-treated cells transfected with mutant *MBTPS2* constructs compared to normal S2P, as detected by western blot analysis (Figure 8B).

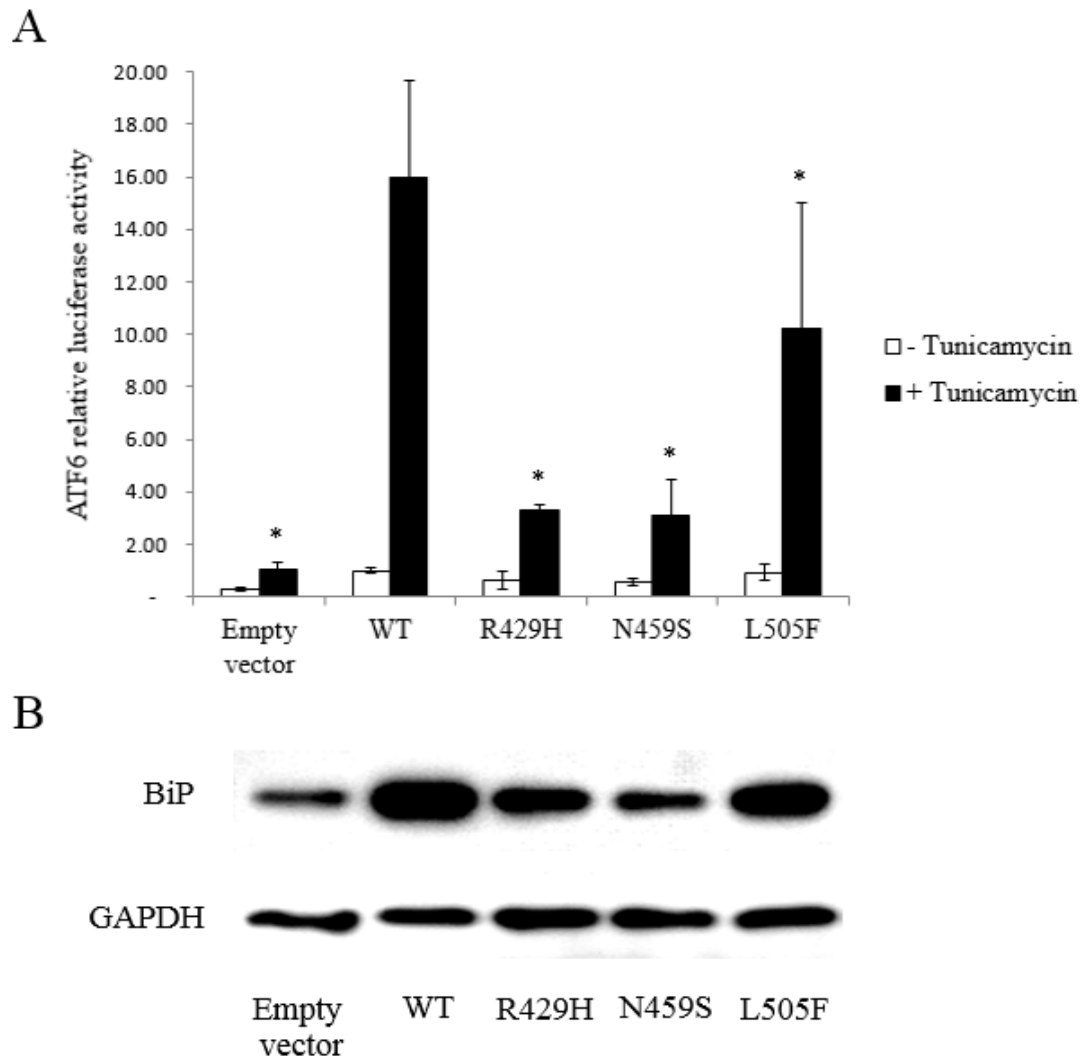


Figure 8. ATF6 transcription activities (A: Luciferase assay, B: BiP protein level, \*:  $p < 0.05$ )

○ CREB3L1

In a direct assay of CREB3L1 (90 kD) cleavage in patients' fibroblasts, 55 kD cleavage products from S1P were increased even in untreated cells and decreased of the 50 kD fragment, that is the cleavage product from S2P. This indicate the decreasing of S2P cleavage activity. (Figure 9). Treatment of cells with ALLN (N-acetyl-leucyl-leucyl-norleucinal) to prevent of degradation of CREB3L1 cleavage products.

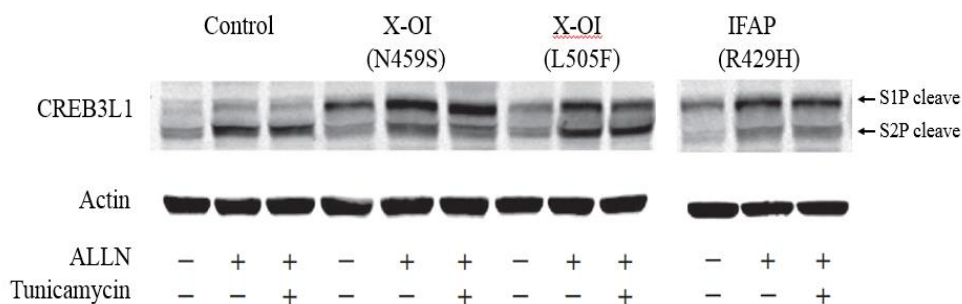


Figure 9. Effect of mutations in S2P's cleavage activity on CREB3L1 (4)

### iPSCs generation

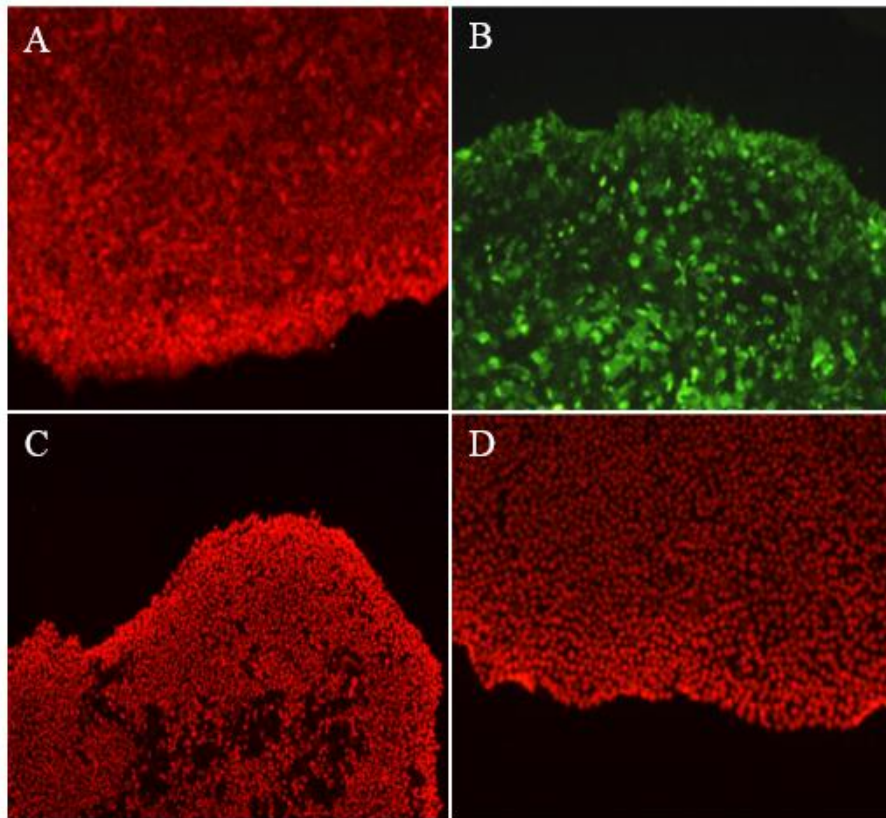
Fibroblasts of patients with X-OI (N459S and L505F) were generated to iPSCs. Yamanaka factors were delivered by non-integrative approaches (sendi virus and episomal vector). We got 7 and 13 clones of iPSCs from X-OI (N459S and L505F). For embryonic stem cells (ESCs) and iPSCs, as control group, the samples were kindly provided by Dr. Ruttachuck Rungsiwiwat (96, 97) (Table 7).

Table 7. Information of stem cells used in this thesis

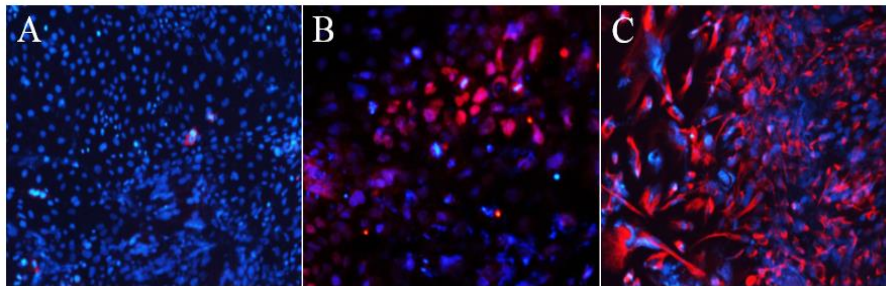
Sample name	Controls		Patients	
	CU	HS4	Thai-XOI	Swiss-XOI
Phenotype	normal	normal	X-OI	X-OI
Genotype	wild type	wild type	N459S	L505F
Cell source	inner cell mass	skin fibroblast	skin fibroblast	skin fibroblast
Delivery system (non-integrative approach)	-	sendi virus	sendi virus	episomal vector
Number of clones	2	2	7	13

### iPSCs Characterization

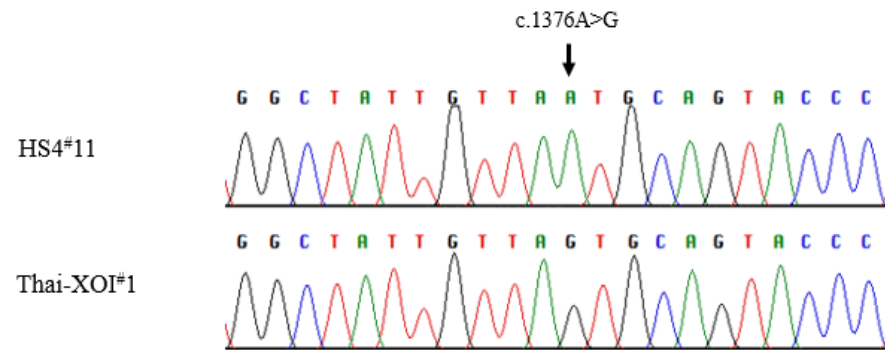
Two clones of each mutation in X-OI were characterized. All of these cells expressed ESC markers and could be differentiated to three germ layers. For karyotype analysis, two clones of Thai X-OI showed inversion at chromosome 9, which is a polymorphism, and the others were normal. Cell identification showed the mutation in each line (Figures 10-13).



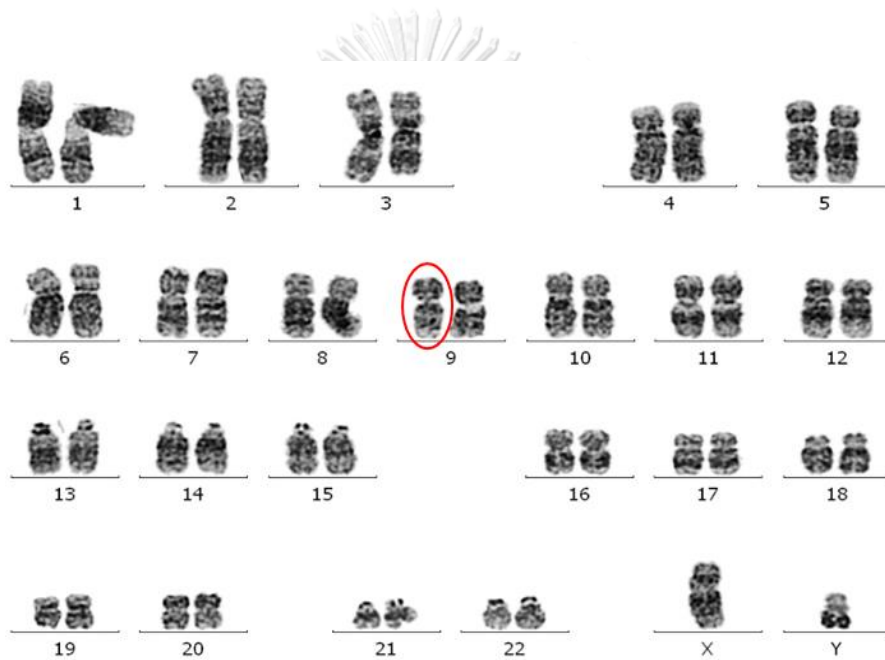
ESC markers (A: SSEA-4, B: TRA-1-60, C: OCT-4, D: NANOG)



Differentiation test (A: endoderm, B: mesoderm, C: ectoderm)

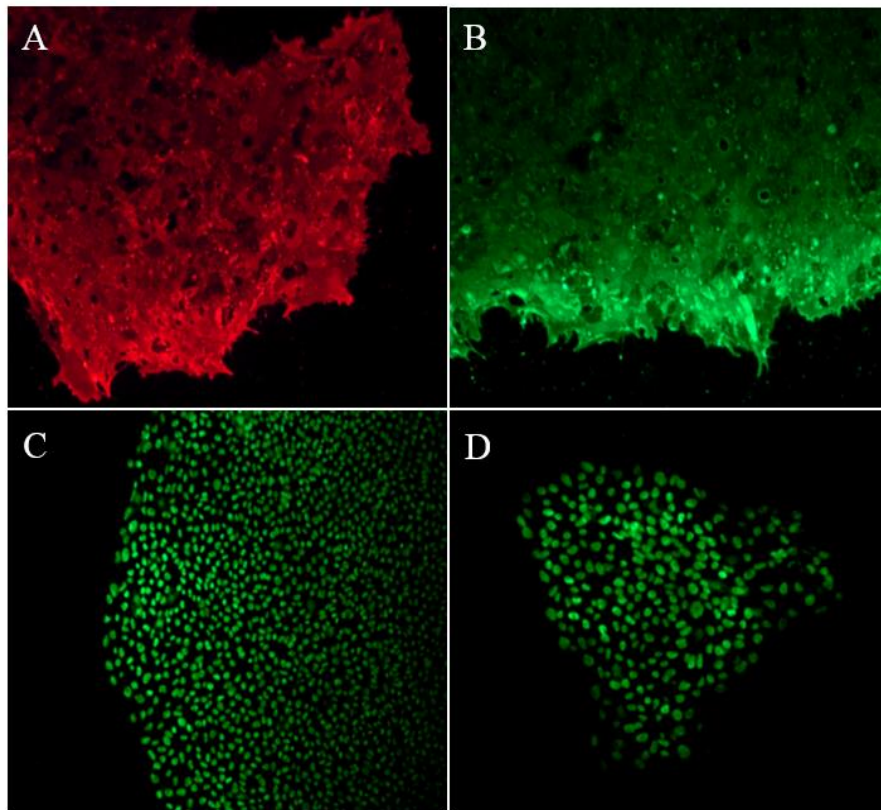


Cell identification

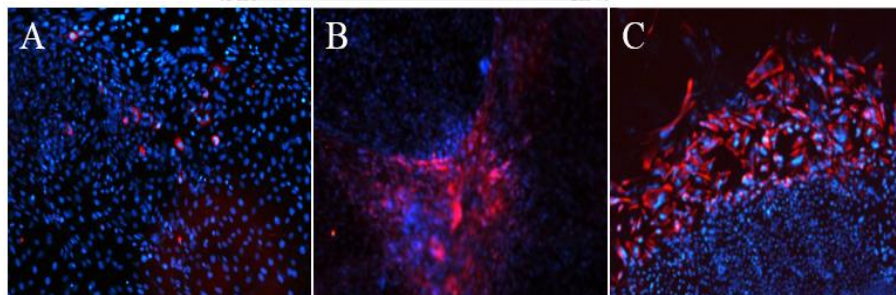


Karyotype analysis: inversion at chromosome 9 (red circle)

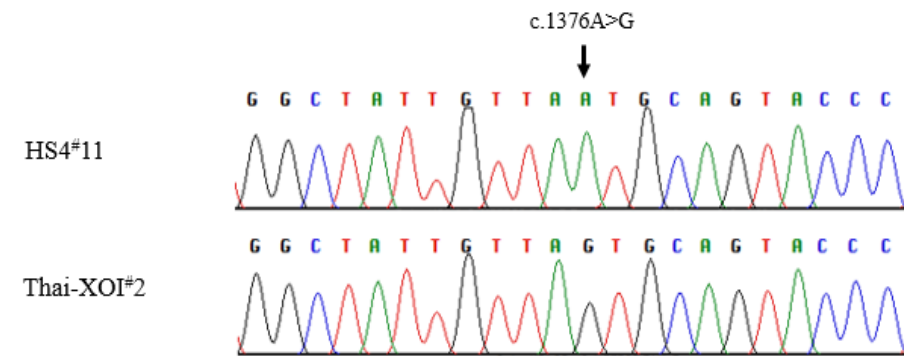
Figure 10. Characterization of Thai X-OI#1



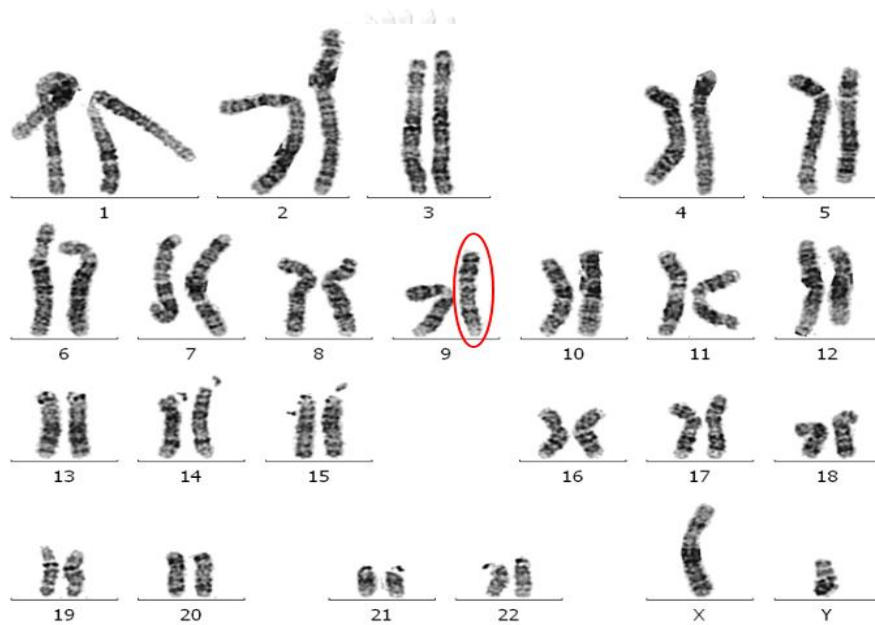
ESC markers (A: SSEA-4, B: TRA-1-60, C: OCT-4, D: NANOG)



Differentiation test (A: endoderm, B: mesoderm, C: ectoderm)

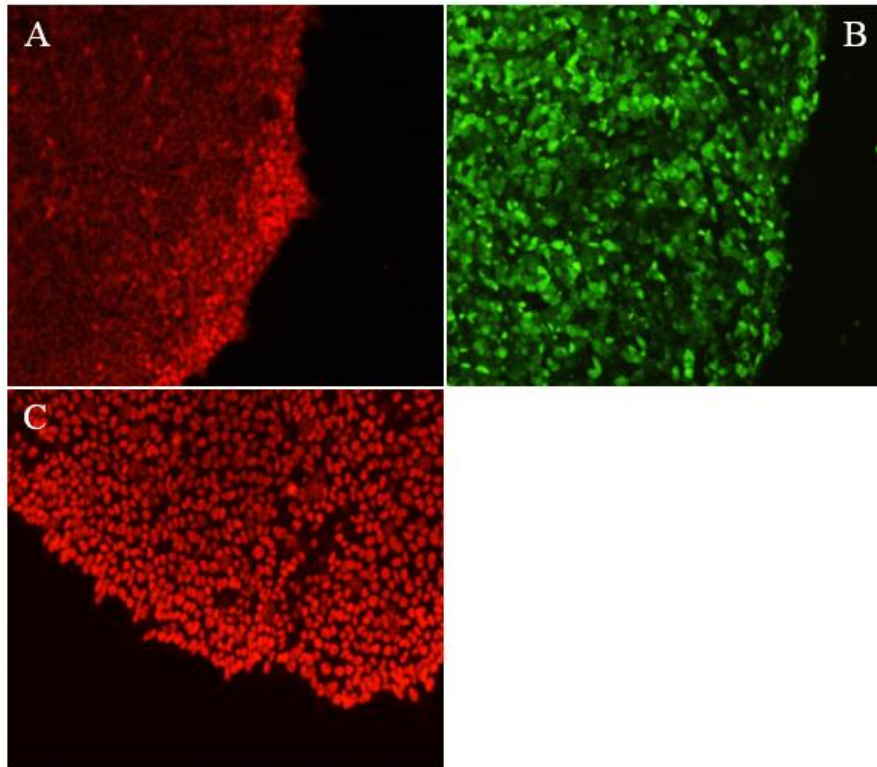


Cell identification

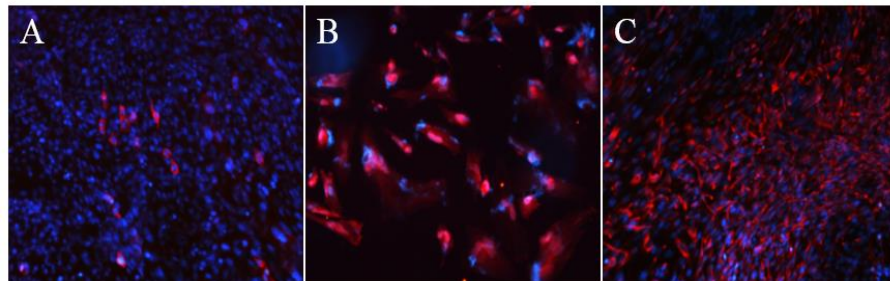


Karyotype analysis: inversion at chromosome 9 (red circle)

Figure 11. Characterization of Thai X-OI#2

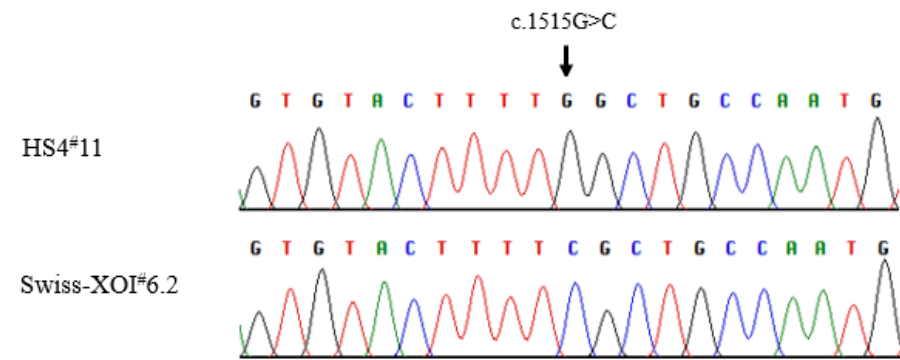


ESC markers (A: SSEA-4, B: TRA-1-60, C: OCT-4)

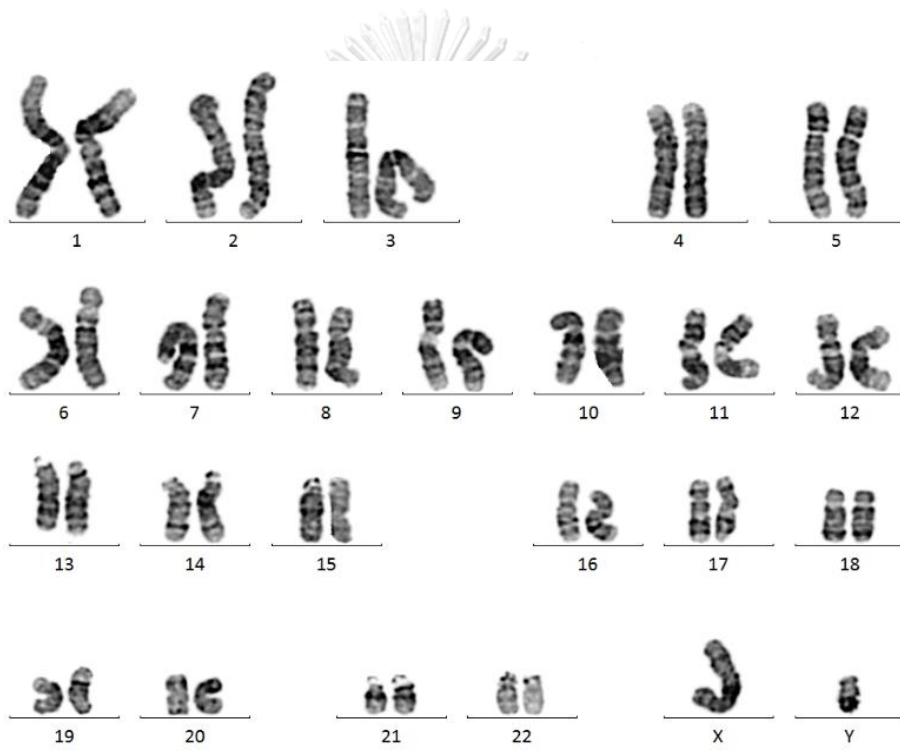


Differentiation test (A: endoderm, B: mesoderm, C: ectoderm)



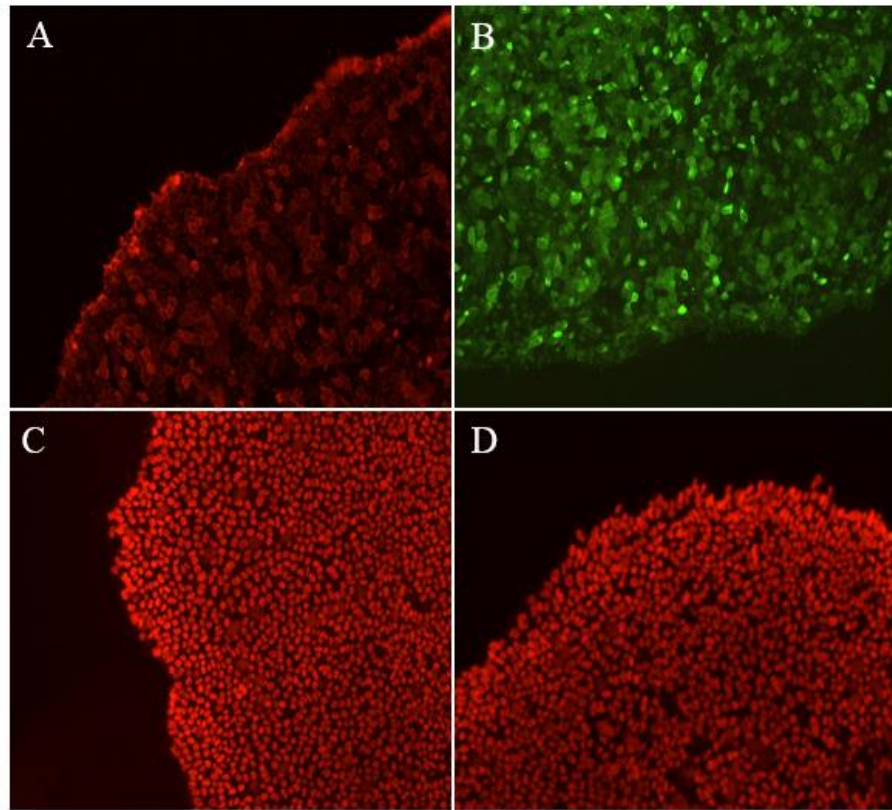


Cell identification

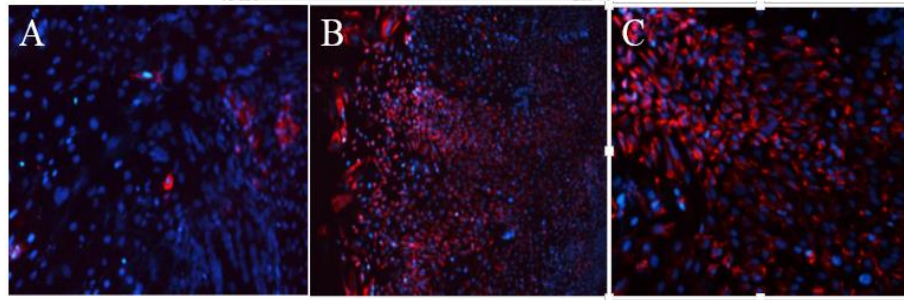


Karyotype analysis

Figure 12. Characterization of Swiss X-OI#6.2



ESC markers (A: SSEA-4, B: TRA-1-60, C: OCT-4, D: NANOG)



Differentiation test (A: endoderm, B: mesoderm, C: ectoderm)

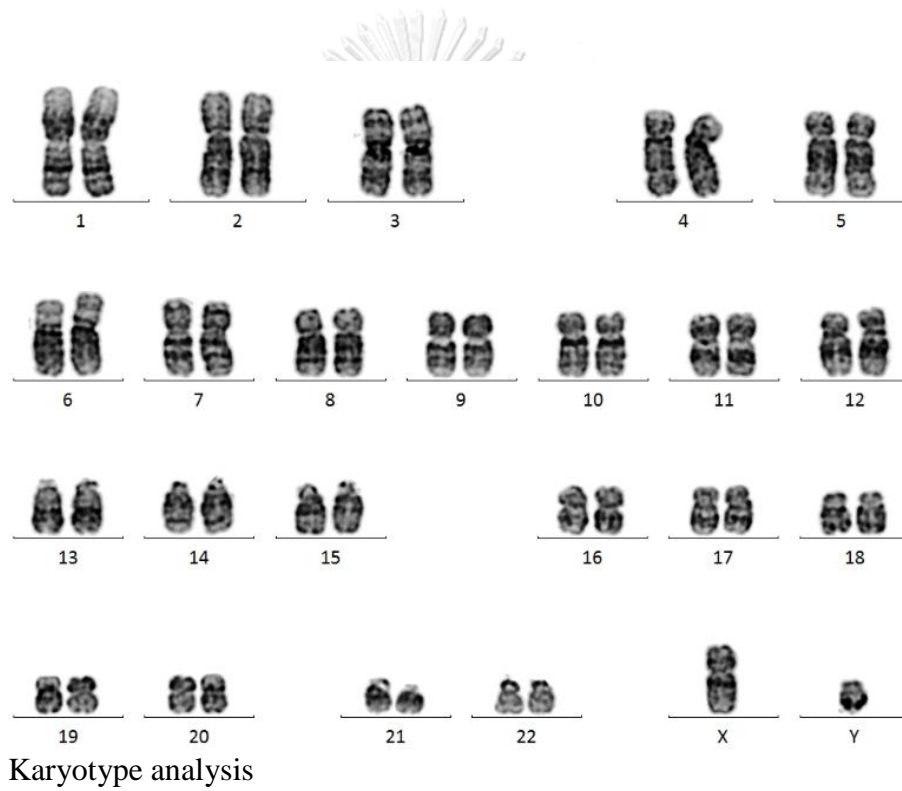
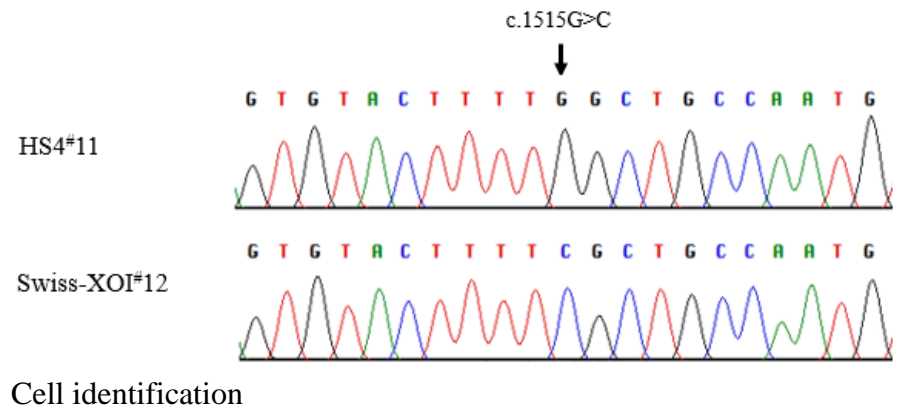


Figure 13. Characterization of Swiss X-OI#12

### iPSCs derived MSCs (iMSCs)

We differentiated iPSCs to MSCs using protocol modified from Hynes, *et al.* (93). After induction iPSCs with MSC differentiation medium, iPSCs slightly morphology changed. Around 2 weeks, group of MSC-like cells were observed. Allowing them to proliferate about 5-7 days, they were dissociated, called passage 0 (P.0) (Figure 14). About passage fourth of iMSCs, cells were homogenous and adhere to non-coated culture dish, that is one of MSC properties. After that, iMSCs were evaluated MSC markers. About 90% of MSC markers showed in each iMSC line, except CD90 (Table 8).

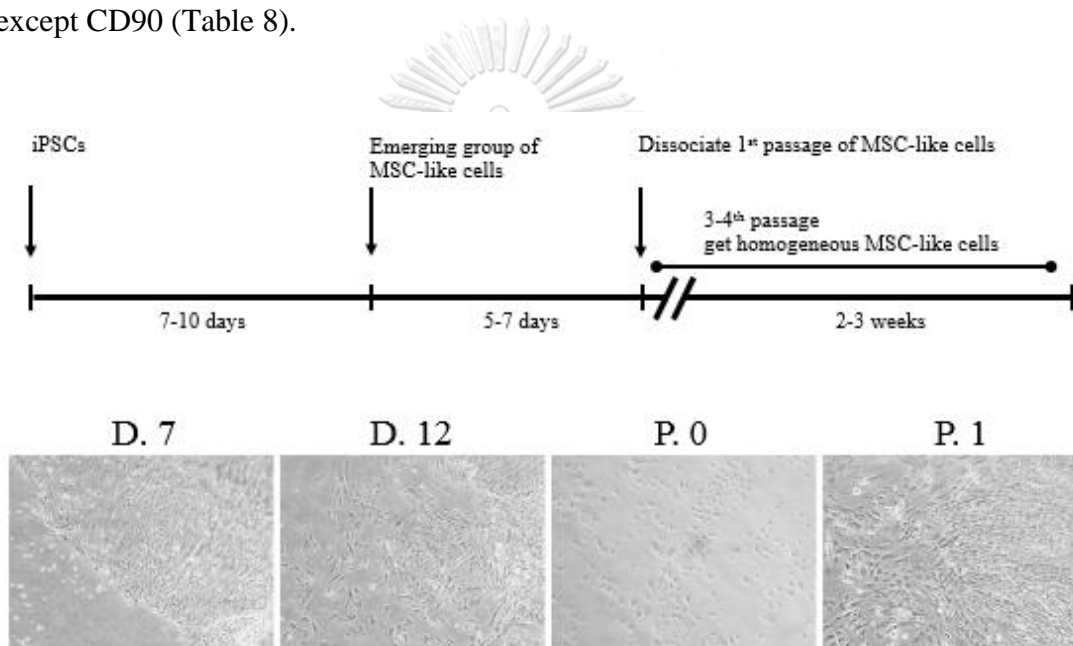


Figure 14. Time line for MSC differentiation

Table 8. MSC markers of iMSCs

Sample	Clone (#)	MSC markers			
		CD44	CD73	CD90	CD105
CU	2	99.9	99.9	88.7	99.9
	4	99.9	100.0	22.4	99.6
HS4	2	99.0	99.8	98.1	96.0
	11	99.9	100.0	29.5	58.1
Thai-XOI	1	99.6	100.0	35.8	99.5
	2	99.6	100.0	94.8	84.6
Swiss-XOI	12	99.8	100.0	23.0	99.8
	6.2	96.2	99.8	64.6	98.2

### **iMSC derived osteoblasts**

We differentiated iMSCs to osteoblast using protocol from Jaiswal, *et al* (94). Around 3-5 day, all of iMSCs clones rapidly proliferated and slightly morphology changed. In control group (CU#4 and HS4#11), calcium deposit can be observed under microscope around day 7-9 after induction with osteogenic medium. About 3-5 days later calcium deposit was found in Thai-XOIs (#1 and #2). Swiss-XOIs (#12 and #6.2) cannot observed calcium deposit although complete osteogenic induction (Figure 15). Calcium deposit, in addition observe under microscope, was also detected by Alizarin red staining at day 14 and 21 after osteogenic induction (Figure 16).

When complete osteogenic induction, calcium deposit showed different pattern between control and Thai-XOI. In controls, calcium deposit spreads throughout the culture dish, while Thai-XOIs showed patchy form of it (Figure 17).

In Swiss-XOI, calcium deposit cannot observed even extended to day 28 and 35. Although calcium deposit cannot be detected, hydroxyapatites, crystal complex of combination of calcium and phosphate, were found in media.

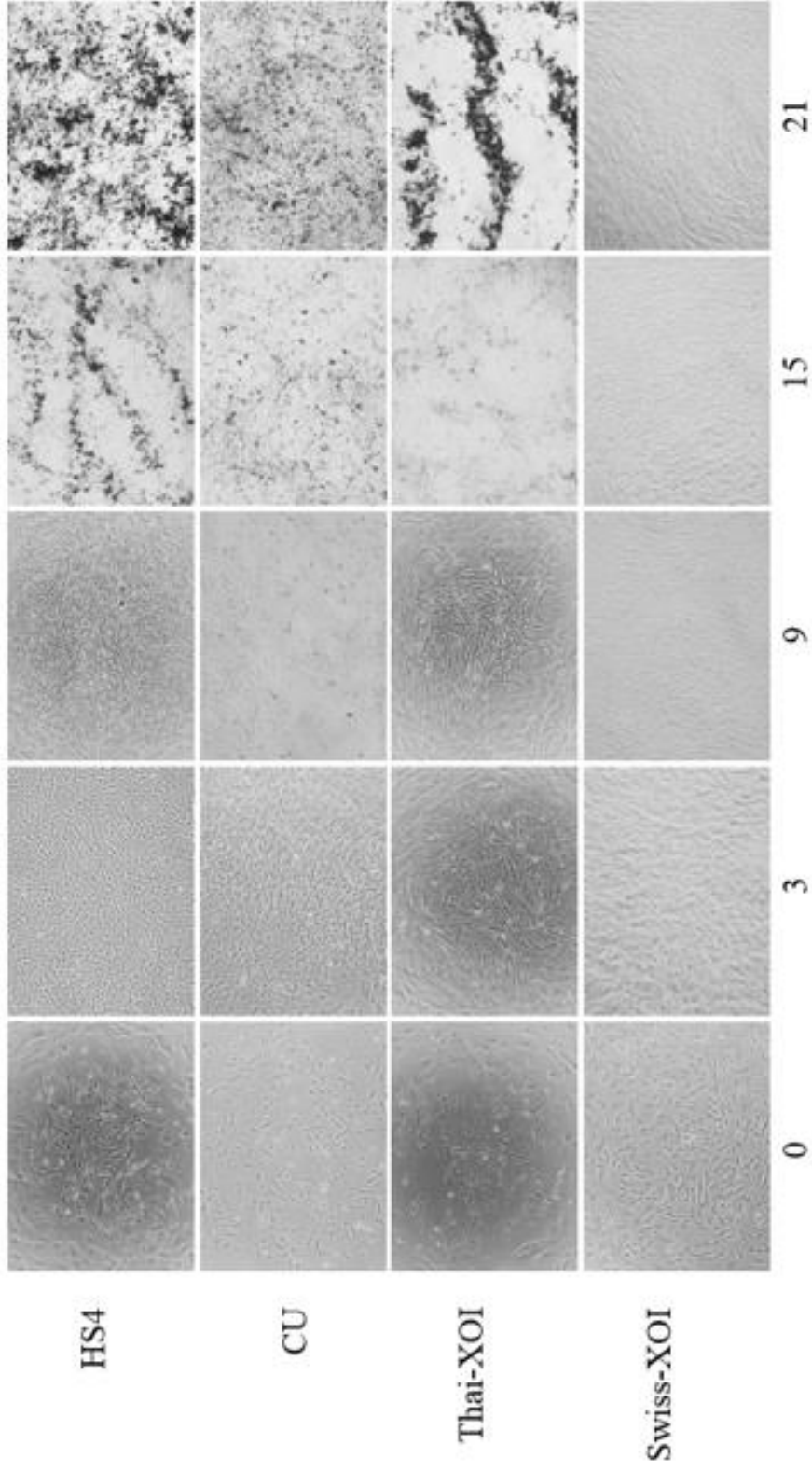


Figure 15. Osteoblast differentiation under microscope at day 0, 3, 9, 15, 21

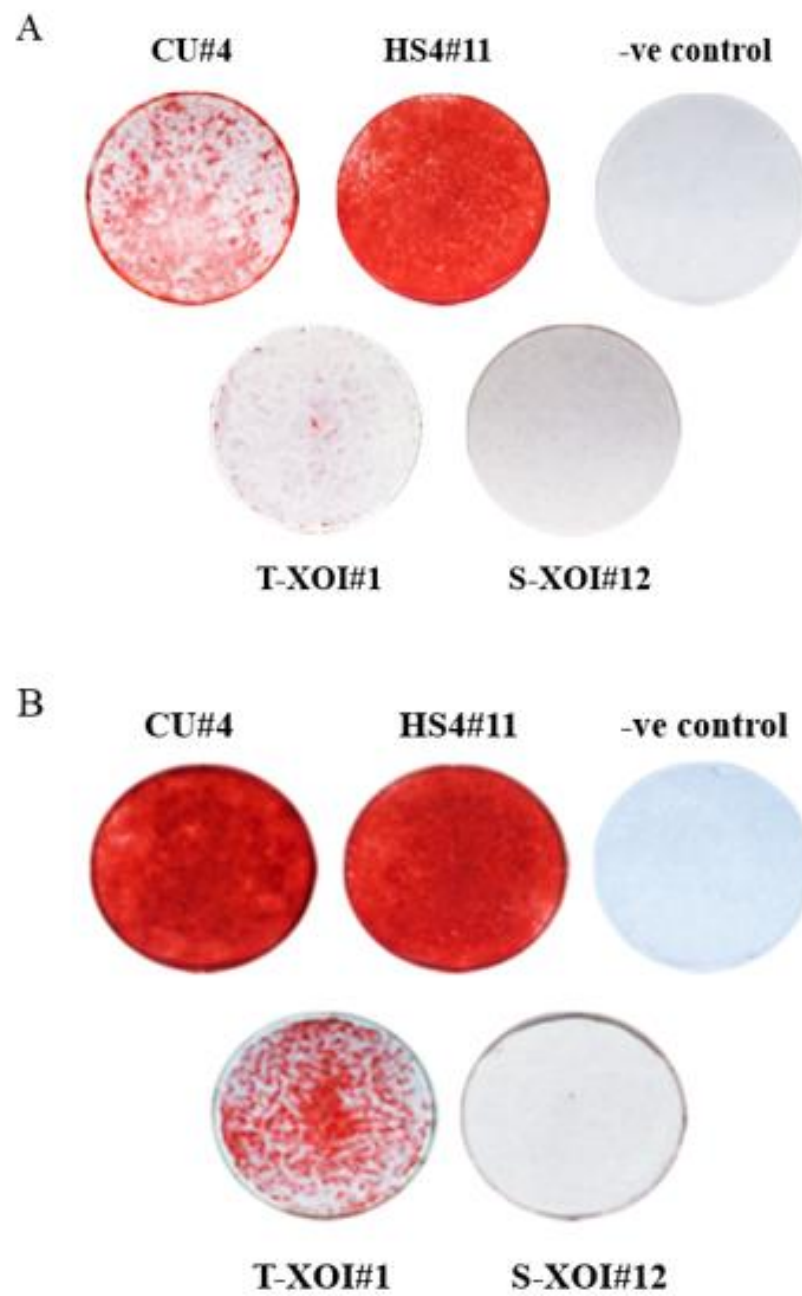


Figure 16. Alizarin red staining at day 14 and 21 after osteogenic induction (A: day 14, B: day 21)

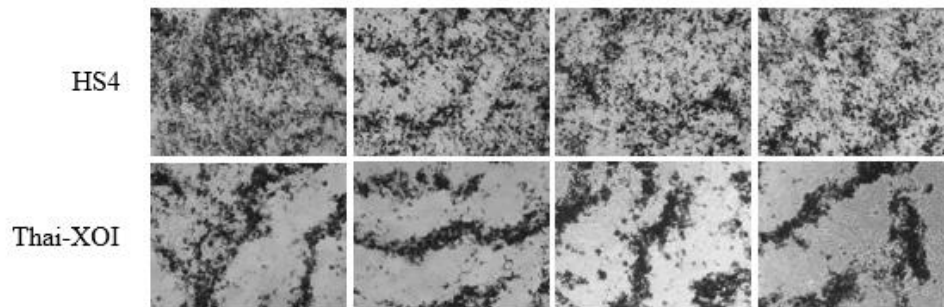
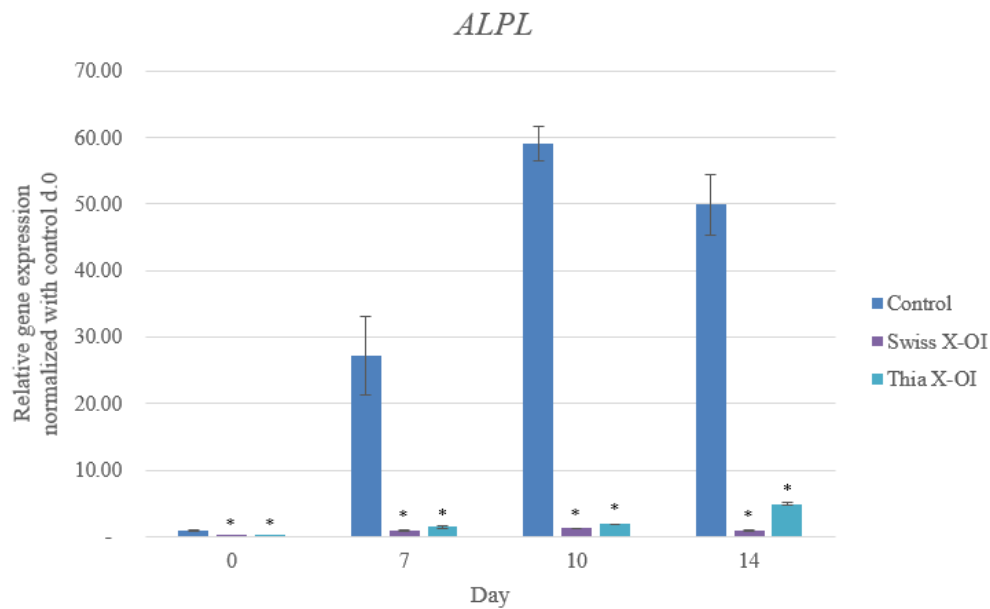


Figure 17. Calcium deposit under microscope at day 21 after osteogenic induction

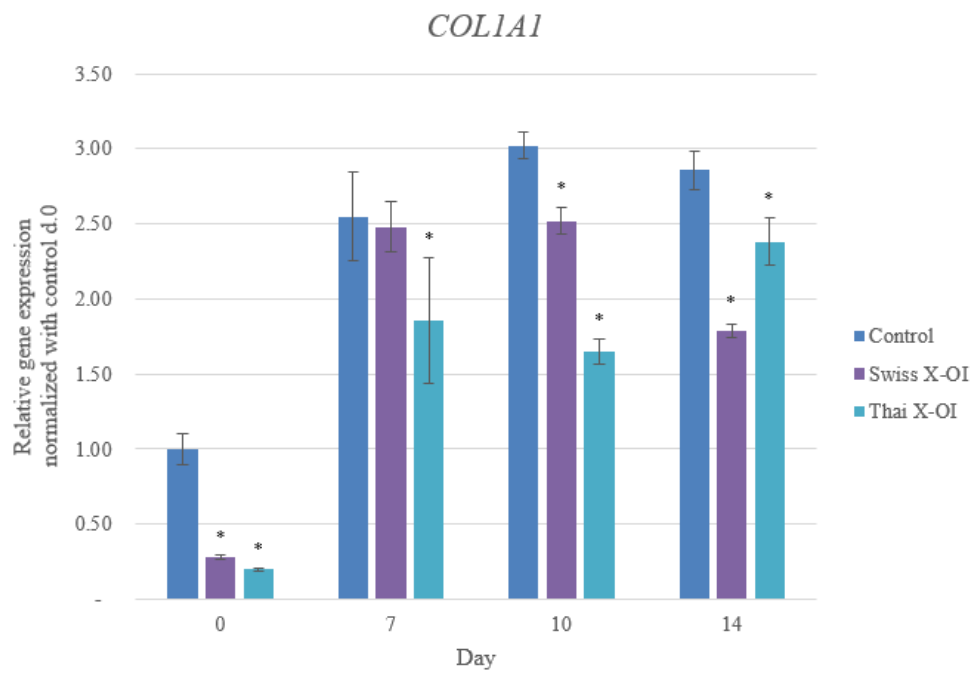
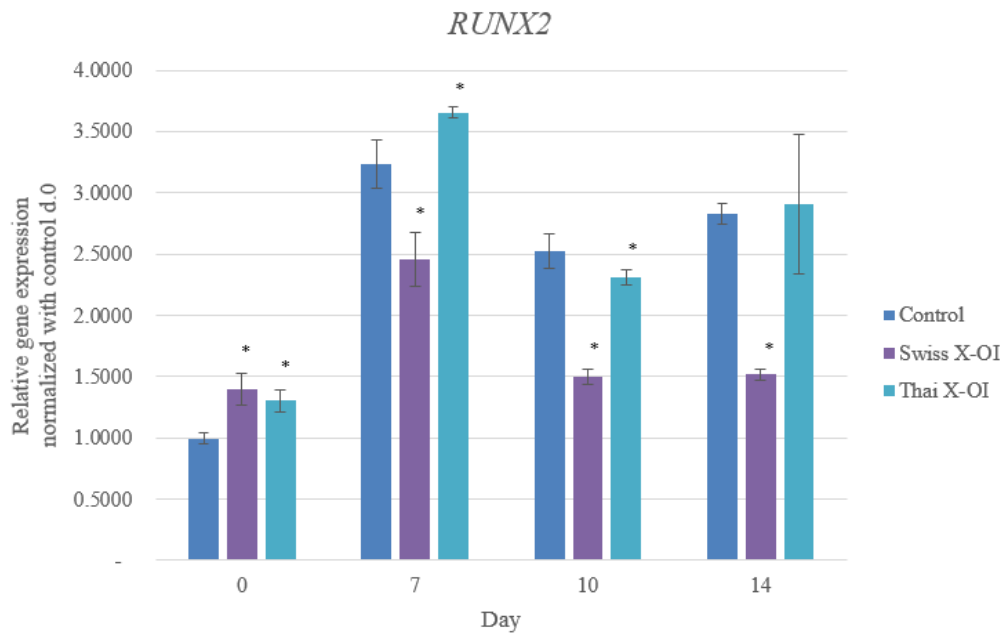
### Gene expression during osteoblast differentiation

#### - Osteogenic markers

Osteogenic markers (*ALPL*, *COL1A1*, *SPP1* and *RUNX2*) were evaluated at day 0, 7, 10 and 14 after osteogenic induction. Comparing to controls, patients' iMSC derived osteoblasts showed low-level expression of *ALPL*, *SPP1* and *COL1A1*. *RUNX2* showed the same level expression in both group (Figure 18).







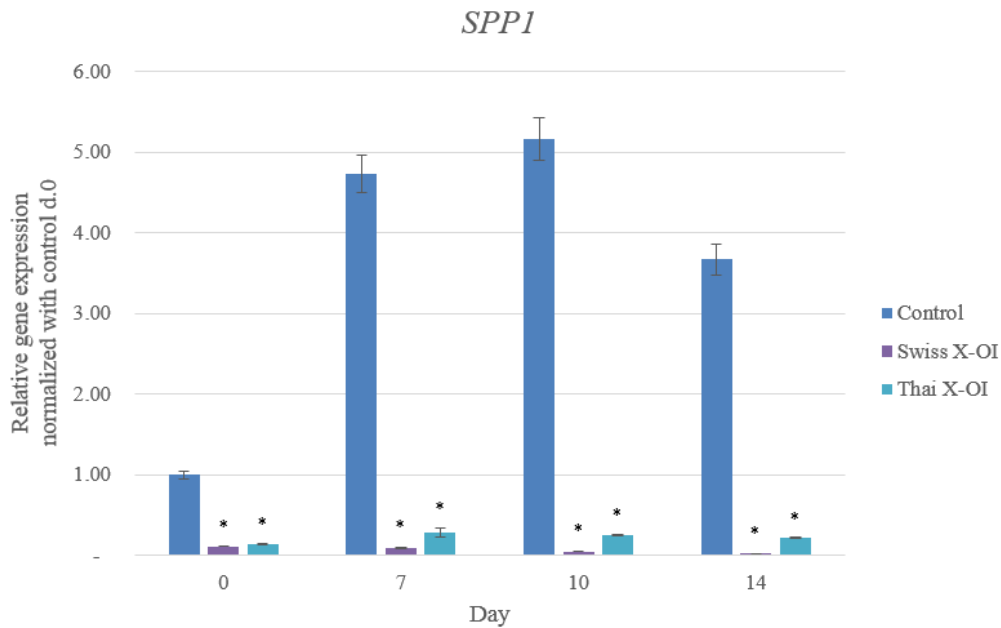


Figure 18. Real time RT-PCR of osteogenic markers, ALPL, COL1A1, RUNX2, and SPP1 genes, in the indicated cell lines after osteogenic differentiation, with GAPDH control (\*:  $p < 0.05$ ).

- Pathomechanism of X-OI

The X-OI's mutations decreased quantity of active form of its targeted proteins, SREBP1, ATF6, CREB3L1 and CREB3L3, so the downstream genes of these could be down regulated. *COL1A1*, *SP7*, *BGLAP*, *LOX*, *SPARC*, *SEC23A* and *SEC24D* are downstream genes of those proteins and involve in osteoblast differentiation. In addition, mutations in *COL1A1*, *SP7* and *SEC24D* cause of OI. With functions of those genes, it is possible to cause of OI phenotype. We investigated gene expression of those genes using real-time RT-PCR. *COL1A1*, *SEC23A*, *SEC24D*, *SPARC* and *LOX* decreased expression comparing to control (Figures 19 and 20).

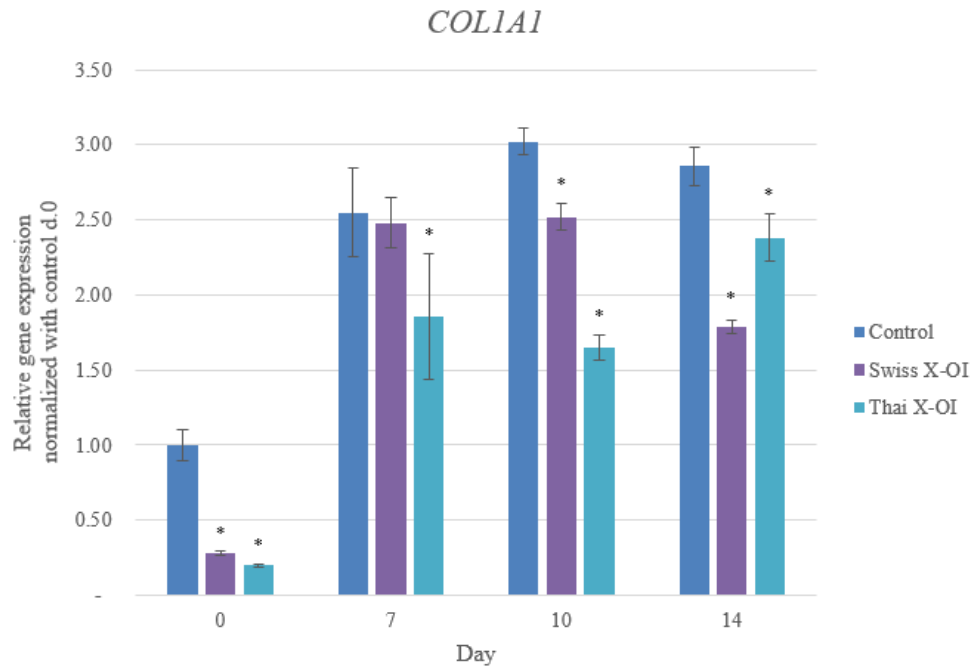
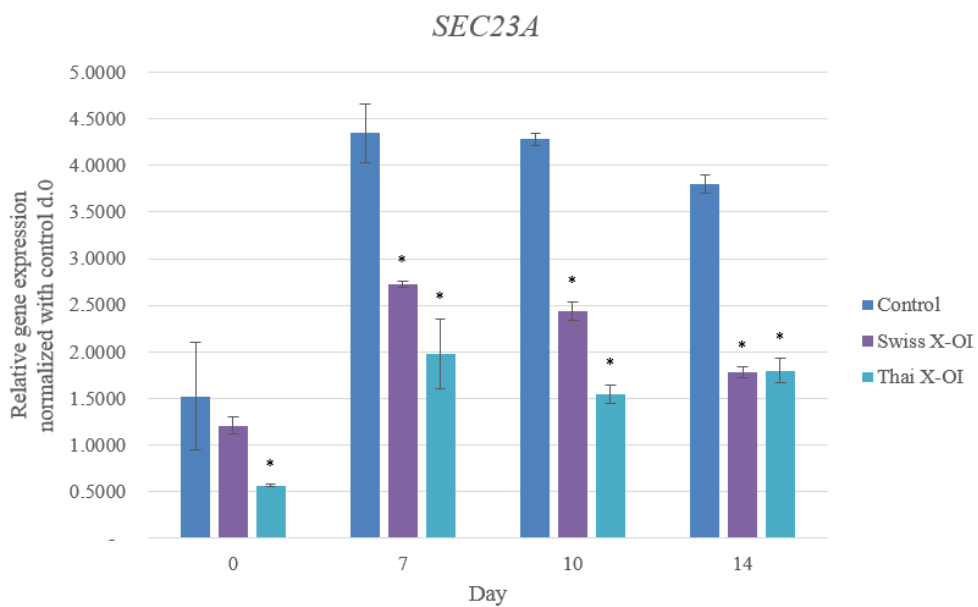
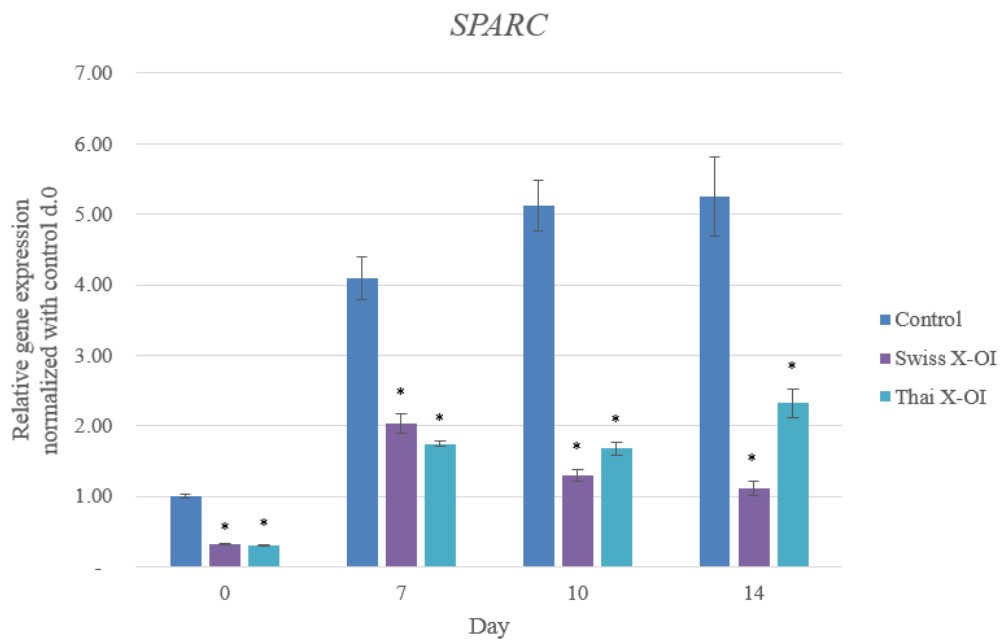
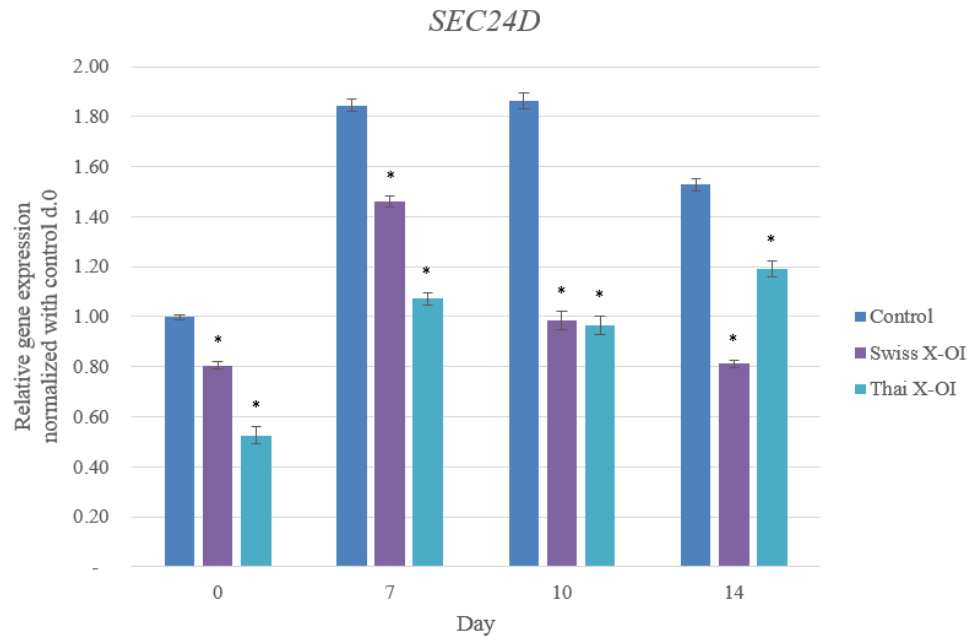


Figure 19. Expression levels of *COL1A1* that induced by CREB3L1 (\*:  $p < 0.05$ )





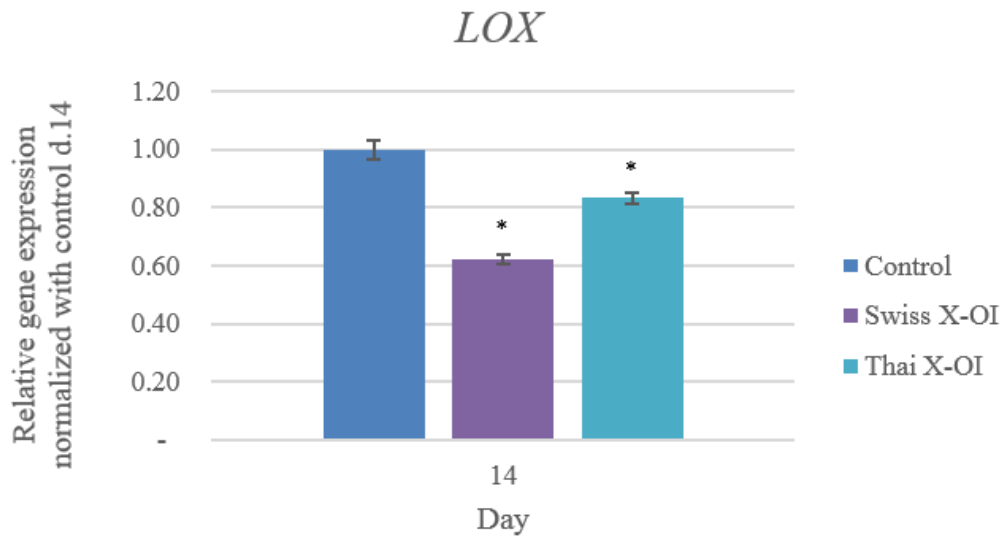


Figure 20. Expression levels of genes (*SEC23A*, *SEC24D*, *SPARC* and *LOX*) that possibly induced by CREB3L3 (\*:  $p < 0.05$ )



## CHAPTER V

### DISCUSSION

Osteogenesis imperfecta exhibits genetic heterogeneity with more than 17 causative genes. All are located on autosomes. We found a large Thai family with many affected patients with a pedigree consistent with an X-linked inheritance. Using many molecular techniques, we successfully identified a novel gene, *MBTPS2*, of osteogenesis imperfecta. *MBTPS2* encodes S2P, a protease cleaving intramembranous protein. It has been previously reported to cause dermatological diseases (9, 11, 12) (IFAP, BERSHECK, KFSDX and Olmsted diseases). Our patients do not have the phenotype overlapping with these diseases. The mutations in our patients located nearly conserved domain, NDPG (48), whereas those mutations of dermatological diseases located throughout the gene (Figure 1). The mutations in X-OI possibly affects specific functions involving in osteoblastogenesis.

S1P and S2P play a role in RIP to liberate intramembranous proteins (SREBP, ATF6 and CREB3 subfamilies) to nucleus where they activate pathways involved in cholesterol homeostasis, unfolded protein response and bone formation. The *MBTPS2* mutations (N459S and L505F) do not affect either the RNA and protein expressions (Figure 7). Instead, they disrupt S2P's cleavage activities of ATF6 and CREB3L1.

We demonstrated that transcriptional activity of ATF6 was decreased in all of CHO-M19 containing mutations (Figure 8). ATF6 functions in osteoblastogenesis. It regulates *SP7* and *BGLAP*. *SP7* is an early marker for osteoblast differentiation and a cause of OI (45, 57, 67). *BGLAP*, extracellular matrix protein, involves in bone mineralization (58). However, homozygous mutations in *ATF6* cause an eye disease, achromatopsia. It is characterized by color blindness, photophobia, nystagmus and severely reduced visual acuity, with no bone defects (70). Thus, ATF6 is unlikely to be a major molecule in the pathomechanical pathway of X-OI.

The effect of mutant S2P in X-OI's fibroblasts showed the decrease of activated CREB3L1 (Figure 9). This might interfere with its downstream functions. Homozygous deletion of *CREB3L1* has been reported to cause bone fragility in mice and severe

recessive OI in human (44, 59). In addition, CREB3L1 has a cell-type specific functions. As previous studies showing CREB3L1 functions relating to the abnormalities in bones, the cell type which we chose to study is bone-producing cells, osteoblasts. Since osteoblasts of the X-OI patients were not available, we opted to generate and study induced pluripotent stem cells (iPSCs).

The patients' fibroblasts were induced to iPSCs by using combination of Yamanaka factors and non-integrative techniques, sendi virus and episomal vector. Two clones of each patient were characterized (Figure 10-13). Then, they were induced to MSCs (iMSCs). Surface markers (CD44, CD73, CD90 and CD105) were used to characterize MSCs. Nearly 90% of them, except CD90, were detected in all iMSCs. For CD90, 20%-100% were found in both groups, controls and patients (Table 7). Although CD90 showed variable expression, all of iMSCs could still differentiate to osteoblasts. However, iMSC groups with low levels of CD90 differentiated to osteoblasts easier than the other groups with high levels of CD90. Recently, it was found that the reduction of CD90 expression enhances osteoblast differentiation of MSCs *in vitro* (98). This is consistent with the observation from our study and supporting the role of CD90 in controlling MSCs differentiation. From this data, CD90 should be evaluated to classify iMSCs into groups before analyzing the result of osteoblast differentiation.

iMSCs were induced to osteoblasts for 21 days. Cells were observed under microscope, calcium deposition were studied by alizarin red staining and RNA expression of various genes were determined by RT-PCR for evaluation of osteoblast differentiation and transcription activities of S2P's target proteins. Cell observation and calcium staining in the Thai X-OI patient showed the delay of calcium deposit (Figure 15) and abnormality of calcium binding (Figure 16). Those of the Swiss X-OI patient showed no detectable calcium deposit, even we extended the differentiation period to 5 weeks (Figures 15 and 16). In addition to the delay or absence of calcium deposit, we found floated HA in X-OI culture media, especially in Swiss X-OI. This indicates that HA can be formed but cannot bind to the matrix. These results indicate that X-OI had defective mineralization.

For gene expression studies, expression levels of each gene were determined using real-time RT-PCR to evaluate osteoblast differentiation and transcription activities of S2P's target proteins. *ALPL*, *SPPI*, *COL1A1* and *RUNX2* are osteogenic

markers to be evaluated for osteoblast differentiation. When comparing to controls, *ALPL*, *SPP1* and *COL1A1* were downregulated whereas *RUNX2* was normal (Figure 18). This suggested that the osteoblast differentiation is defective in X-OI patients.

To evaluate functions of S2P's target proteins, the RNA levels of *COL1A1*, *SPARC*, *SEC23A*, *SEC24D* and *LOX* were determined. Strikingly, all of them were downregulated comparing to controls (Figures 19 and 20). In osteoblasts, *COL1A1* is regulated by CREB3L1. Thus, the decreased expression level of *COL1A1* is possibly resulted from the defective CREB3L1 activation. For *SPARC*, *SEC23A*, *SEC24D* and *LOX*, a previous report showed that overexpression of CREB3L3 led to an upregulation of those genes. In addition, overexpression of CREB3L3 in S1P deficient cells was previously reported to rescue mineralization. This suggested that these genes are downstream genes of CREB3L3 and involved in mineralization (80). Furthermore, *SPARC* and *SEC24D* are causative genes for OI. Taken together, we conclude that the downregulation of those genes possibly causes defective mineralization leading to bone fragility in X-OI patients.

Interestingly, the results from cell observation, calcium staining and gene expression studies support one another. First, the delay or absence of calcium deposit is consistent with down regulated of *ALPL*, *SPP1* and *SPARC*, which are involved in bone mineralization. *ALPL* hydrolyzes inorganic pyrophosphate (PPi) to inorganic phosphate (Pi) that is an initiate substrate to form HA. Its downregulation possibly led to delay of HA formation supporting the delay of calcium deposit. *SPP1* could either induce or inhibit mineralization depending on its phosphorylation state. It were downregulated in early osteoblast differentiation affecting the delay of calcium deposit (99). *SPARC* or osteonectin is a bone-specific protein linking collagen and HA (100). With the decrease of *SPARC* expression, possibly reduced binding of HA to collagen. In addition, animal model study showed the decreased mineralized nodules in osteonectin-null mice, consistent with our results (101). Furthermore, *SPARC* causes a recessive OI. Like our patients, the patients with mutations in *SPARC* showed the decreased secretion of collagen type I. However, they were found to have over-modification of alpha chain of type I collagen. This differs from our patients (20). From these data, combination of the decreased expression of *ALPL*, *SPP1* and *SPARC* might cause a defect in mineralization. Second, the floated HA in X-OI culture media supports



the delay and absence of calcium deposit and is consistent with the decreased expression of *SPARC* in our patients. With decreased *SPARC*, HA possibly reduced binding to collagen. Then, the residual HA that did not bind to collagen floated in culture media. Third, abnormalities of calcium binding might result from the downregulated *COL1A1* expression and decreased secretion of collagen type I (reported by Lindert, *et al.*). The same pattern was found in type V OI. Osteoblasts of patients with *IFITM5*, the causative gene of type V OI, showed the decrease of *COL1A1* expression and secretion while increase of mineralization. Decreasing collagen type I secretion changed the collagen formation in matrix. It showed a patchy form that was observed in the Thai X-OI patient (102). From these data, we concluded that X-OI patients have defects in osteoblast differentiation and mineralization that cause bone fragility, an important characteristic in OI.

We found the possible mechanisms leading to patients with X-OI containing mutations, p.N459S and L505F, in *MBTPS2*. The defective cleavage of CREB3L1, potentially leading to decreased *COL1A1* expression, which in turn could contribute to bone fragility. In addition, mutant *MBTPS2* may lead to defective cleavage of CREB3L3, which might be the cause of downregulations of *SEC23A*, *SEC24D*, *SPARC* and *LOX*. In summary, we generated patients specific skin fibroblast-derived iPSCs and then derived to osteoblasts, which lead us to a working hypothesis that mutant *MBTPS2* may lead to defective cleavages of CREB3L1 and CREB3L3, decreasing expressions of *COL1A1*, *SEC23A*, *SEC24D*, *SPARC* and *LOX*, resulting in bone fragility in X-linked OI.

## REFERENCES

1. Kang H, Aryal ACS, Marini JC. Osteogenesis imperfecta: new genes reveal novel mechanisms in bone dysplasia. *Translational research : the journal of laboratory and clinical medicine*. 2017;181:27-48.
2. Forlino A, Marini JC. Osteogenesis imperfecta. *Lancet*. 2016;387(10028):1657-71.
3. Marini JC, Forlino A, Bachinger HP, Bishop NJ, Byers PH, Paepe A, et al. Osteogenesis imperfecta. *Nature reviews Disease primers*. 2017;3:17052.
4. Lindert U, Cabral WA, Ausavarat S, Tongkobpetch S, Ludin K, Barnes AM, et al. MBTPS2 mutations cause defective regulated intramembrane proteolysis in X-linked osteogenesis imperfecta. *Nature communications*. 2016;7:11920.
5. Lal M, Caplan M. Regulated intramembrane proteolysis: signaling pathways and biological functions. *Physiology*. 2011;26(1):34-44.
6. Murakami T, Kondo S, Ogata M, Kanemoto S, Saito A, Wanaka A, et al. Cleavage of the membrane-bound transcription factor OASIS in response to endoplasmic reticulum stress. *Journal of neurochemistry*. 2006;96(4):1090-100.
7. Ye J, Rawson RB, Komuro R, Chen X, Dave UP, Prywes R, et al. ER stress induces cleavage of membrane-bound ATF6 by the same proteases that process SREBPs. *Molecular cell*. 2000;6(6):1355-64.
8. Wang X, Sato R, Brown MS, Hua X, Goldstein JL. SREBP-1, a membrane-bound transcription factor released by sterol-regulated proteolysis. *Cell*. 1994;77(1):53-62.
9. Haghghi A, Scott CA, Poon DS, Yaghoobi R, Saleh-Gohari N, Plagnol V, et al. A missense mutation in the MBTPS2 gene underlies the X-linked form of Olmsted syndrome. *The Journal of investigative dermatology*. 2013;133(2):571-3.
10. Naiki M, Mizuno S, Yamada K, Yamada Y, Kimura R, Oshiro M, et al. MBTPS2 mutation causes BRESEK/BRESHECK syndrome. *American journal of medical genetics Part A*. 2012;158A(1):97-102.
11. Aten E, Brasz LC, Bornholdt D, Hooijkaas IB, Porteous ME, Sybert VP, et al. Keratosis Follicularis Spinulosa Decalvans is caused by mutations in MBTPS2. *Human mutation*. 2010;31(10):1125-33.
12. Oeffner F, Fischer G, Happel R, Konig A, Betz RC, Bornholdt D, et al. IFAP syndrome is caused by deficiency in MBTPS2, an intramembrane zinc metalloprotease essential for cholesterol homeostasis and ER stress response. *American journal of human genetics*. 2009;84(4):459-67.
13. Sillence DO, Senn A, Danks DM. Genetic heterogeneity in osteogenesis imperfecta. *Journal of medical genetics*. 1979;16(2):101-16.
14. Pope FM, Nicholls AC, McPheat J, Talmud P, Owen R. Collagen genes and proteins in osteogenesis imperfecta. *Journal of medical genetics*. 1985;22(6):466-78.
15. Becker J, Semler O, Gilissen C, Li Y, Bolz HJ, Giunta C, et al. Exome sequencing identifies truncating mutations in human SERPINF1 in autosomal-recessive osteogenesis imperfecta. *American journal of human genetics*. 2011;88(3):362-71.
16. Shaheen R, Alazami AM, Alshammari MJ, Faqeih E, Alhashmi N, Mousa N, et al. Study of autosomal recessive osteogenesis imperfecta in Arabia reveals a novel

locus defined by TMEM38B mutation. *Journal of medical genetics*. 2012;49(10):630-5.

17. Cho TJ, Lee KE, Lee SK, Song SJ, Kim KJ, Jeon D, et al. A single recurrent mutation in the 5'-UTR of IFITM5 causes osteogenesis imperfecta type V. *American journal of human genetics*. 2012;91(2):343-8.

18. Fahiminiya S, Majewski J, Mort J, Moffatt P, Glorieux FH, Rauch F. Mutations in WNT1 are a cause of osteogenesis imperfecta. *Journal of medical genetics*. 2013;50(5):345-8.

19. Garbes L, Kim K, Riess A, Hoyer-Kuhn H, Beleggia F, Bevot A, et al. Mutations in SEC24D, encoding a component of the COPII machinery, cause a syndromic form of osteogenesis imperfecta. *American journal of human genetics*. 2015;96(3):432-9.

20. Mendoza-Londono R, Fahiminiya S, Majewski J, Care4Rare Canada C, Tetreault M, Nadaf J, et al. Recessive osteogenesis imperfecta caused by missense mutations in SPARC. *American journal of human genetics*. 2015;96(6):979-85.

21. Forlino A, Cabral WA, Barnes AM, Marini JC. New perspectives on osteogenesis imperfecta. *Nature reviews Endocrinology*. 2011;7(9):540-57.

22. Willing MC, Deschenes SP, Slayton RL, Roberts EJ. Premature chain termination is a unifying mechanism for COL1A1 null alleles in osteogenesis imperfecta type I cell strains. *American journal of human genetics*. 1996;59(4):799-809.

23. Redford-Badwal DA, Stover ML, Valli M, McKinstry MB, Rowe DW. Nuclear retention of COL1A1 messenger RNA identifies null alleles causing mild osteogenesis imperfecta. *The Journal of clinical investigation*. 1996;97(4):1035-40.

24. Genovese C, Rowe D. Analysis of cytoplasmic and nuclear messenger RNA in fibroblasts from patients with type I osteogenesis imperfecta. *Methods in enzymology*. 1987;145:223-35.

25. van Dijk FS, Nesbitt IM, Zwikstra EH, Nikkels PG, Piersma SR, Fratantoni SA, et al. PPIB mutations cause severe osteogenesis imperfecta. *American journal of human genetics*. 2009;85(4):521-7.

26. Morello R, Bertin TK, Chen Y, Hicks J, Tonachini L, Monticone M, et al. CRTAP is required for prolyl 3-hydroxylation and mutations cause recessive osteogenesis imperfecta. *Cell*. 2006;127(2):291-304.

27. Vranka JA, Sakai LY, Bachinger HP. Prolyl 3-hydroxylase 1, enzyme characterization and identification of a novel family of enzymes. *The Journal of biological chemistry*. 2004;279(22):23615-21.

28. Pyott SM, Schwarze U, Christiansen HE, Pepin MG, Leistriz DF, Dineen R, et al. Mutations in PPIB (cyclophilin B) delay type I procollagen chain association and result in perinatal lethal to moderate osteogenesis imperfecta phenotypes. *Human molecular genetics*. 2011;20(8):1595-609.

29. Hudson DM, Kim LS, Weis M, Cohn DH, Eyre DR. Peptidyl 3-hydroxyproline binding properties of type I collagen suggest a function in fibril supramolecular assembly. *Biochemistry*. 2012;51(12):2417-24.

30. Ishikawa Y, Wirz J, Vranka JA, Nagata K, Bachinger HP. Biochemical characterization of the prolyl 3-hydroxylase 1 cartilage-associated protein-cyclophilin B complex. *The Journal of biological chemistry*. 2009;284(26):17641-7.

31. Steinlein OK, Aichinger E, Trucks H, Sander T. Mutations in FKBP10 can cause a severe form of isolated Osteogenesis imperfecta. *BMC medical genetics*. 2011;12:152.
32. Christiansen HE, Schwarze U, Pyott SM, AlSwaied A, Al Balwi M, Alrasheed S, et al. Homozygosity for a missense mutation in SERPINH1, which encodes the collagen chaperone protein HSP47, results in severe recessive osteogenesis imperfecta. *American journal of human genetics*. 2010;86(3):389-98.
33. Koide T, Nishikawa Y, Asada S, Yamazaki CM, Takahara Y, Homma DL, et al. Specific recognition of the collagen triple helix by chaperone HSP47. II. The HSP47-binding structural motif in collagens and related proteins. *The Journal of biological chemistry*. 2006;281(16):11177-85.
34. Ishikawa Y, Vranka J, Wirz J, Nagata K, Bachinger HP. The rough endoplasmic reticulum-resident FK506-binding protein FKBP65 is a molecular chaperone that interacts with collagens. *The Journal of biological chemistry*. 2008;283(46):31584-90.
35. McPherson E, Clemens M. Bruck syndrome (osteogenesis imperfecta with congenital joint contractures): review and report on the first North American case. *American journal of medical genetics*. 1997;70(1):28-31.
36. Eyre DR, Weis MA. Bone collagen: new clues to its mineralization mechanism from recessive osteogenesis imperfecta. *Calcified tissue international*. 2013;93(4):338-47.
37. Eyre DR, Koob TJ, Van Ness KP. Quantitation of hydroxypyridinium crosslinks in collagen by high-performance liquid chromatography. *Analytical biochemistry*. 1984;137(2):380-8.
38. Puig-Hervas MT, Temtamy S, Aglan M, Valencia M, Martinez-Glez V, Ballesta-Martinez MJ, et al. Mutations in PLOD2 cause autosomal-recessive connective tissue disorders within the Bruck syndrome--osteogenesis imperfecta phenotypic spectrum. *Human mutation*. 2012;33(10):1444-9.
39. Schwarze U, Cundy T, Pyott SM, Christiansen HE, Hegde MR, Bank RA, et al. Mutations in FKBP10, which result in Bruck syndrome and recessive forms of osteogenesis imperfecta, inhibit the hydroxylation of telopeptide lysines in bone collagen. *Human molecular genetics*. 2013;22(1):1-17.
40. Martinez-Glez V, Valencia M, Caparros-Martin JA, Aglan M, Temtamy S, Tenorio J, et al. Identification of a mutation causing deficient BMP1/mTLD proteolytic activity in autosomal recessive osteogenesis imperfecta. *Human mutation*. 2012;33(2):343-50.
41. Lindahl K, Barnes AM, Fratzi-Zelman N, Whyte MP, Hefferan TE, Makareeva E, et al. COL1 C-propeptide cleavage site mutations cause high bone mass osteogenesis imperfecta. *Human mutation*. 2011;32(6):598-609.
42. Zhang H, Yue H, Wang C, Gu J, He J, Fu W, et al. Novel mutations in the SEC24D gene in Chinese families with autosomal recessive osteogenesis imperfecta. *Osteoporosis international : a journal established as result of cooperation between the European Foundation for Osteoporosis and the National Osteoporosis Foundation of the USA*. 2017;28(4):1473-80.
43. Moosa S, Chung BH, Tung JY, Altmuller J, Thiele H, Nurnberg P, et al. Mutations in SEC24D cause autosomal recessive osteogenesis imperfecta. *Clinical genetics*. 2015.

44. Symoens S, Malfait F, D'Hondt S, Callewaert B, Dheedene A, Steyaert W, et al. Deficiency for the ER-stress transducer OASIS causes severe recessive osteogenesis imperfecta in humans. *Orphanet journal of rare diseases*. 2013;8:154.
45. Lapunzina P, Aglan M, Temtamy S, Caparros-Martin JA, Valencia M, Leton R, et al. Identification of a frameshift mutation in Osterix in a patient with recessive osteogenesis imperfecta. *American journal of human genetics*. 2010;87(1):110-4.
46. Farber CR, Reich A, Barnes AM, Becerra P, Rauch F, Cabral WA, et al. A novel IFITM5 mutation in severe atypical osteogenesis imperfecta type VI impairs osteoblast production of pigment epithelium-derived factor. *Journal of bone and mineral research : the official journal of the American Society for Bone and Mineral Research*. 2014;29(6):1402-11.
47. Li F, Armstrong GB, Tombran-Tink J, Niyibizi C. Pigment epithelium derived factor upregulates expression of vascular endothelial growth factor by human mesenchymal stem cells: Possible role in PEDF regulated matrix mineralization. *Biochemical and biophysical research communications*. 2016;478(3):1106-10.
48. Rudner DZ, Fawcett P, Losick R. A family of membrane-embedded metalloproteases involved in regulated proteolysis of membrane-associated transcription factors. *Proceedings of the National Academy of Sciences of the United States of America*. 1999;96(26):14765-70.
49. Kinch LN, Ginalski K, Grishin NV. Site-2 protease regulated intramembrane proteolysis: sequence homologs suggest an ancient signaling cascade. *Protein science : a publication of the Protein Society*. 2006;15(1):84-93.
50. Bornholdt D, Atkinson TP, Bouadjar B, Catteau B, Cox H, De Silva D, et al. Genotype-Phenotype Correlations Emerging from the Identification of Missense Mutations in MBTPS2. *Human mutation*. 2013.
51. Fong K, Wedgeworth EK, Lai-Cheong JE, Tosi I, Mellerio JE, Powell AM, et al. MBTPS2 mutation in a British pedigree with keratosis follicularis spinulosa decalvans. *Clinical and experimental dermatology*. 2012;37(6):631-4.
52. Pietrzak A, Kanitakis J, Staskiewicz G, Sobczynska-Tomaszewska A, Dybiec E, Szumilo J, et al. IFAP syndrome with severe cutaneous, neurologic and skeletal manifestations due to a novel MBTPS2 mutation in a Polish patient. *European journal of dermatology : EJD*. 2012;22(4):467-72.
53. Tang L, Liang J, Wang W, Yu L, Yao Z. A novel mutation in MBTPS2 causes a broad phenotypic spectrum of ichthyosis follicularis, atrichia, and photophobia syndrome in a large Chinese family. *Journal of the American Academy of Dermatology*. 2011;64(4):716-22.
54. Nakayama J, Iwasaki N, Shin K, Sato H, Kamo M, Ohyama M, et al. A Japanese case of ichthyosis follicularis with atrichia and photophobia syndrome with an MBTPS2 mutation. *Journal of human genetics*. 2011;56(3):250-2.
55. Ding YG, Wang JY, Qiao JJ, Mao XH, Cai SQ. A novel mutation in MBTPS2 causes ichthyosis follicularis, alopecia and photophobia (IFAP) syndrome in a Chinese family. *The British journal of dermatology*. 2010;163(4):886-9.
56. Rawson RB, Zelenski NG, Nijhawan D, Ye J, Sakai J, Hasan MT, et al. Complementation cloning of S2P, a gene encoding a putative metalloprotease required for intramembrane cleavage of SREBPs. *Molecular cell*. 1997;1(1):47-57.

57. Tohmonda T, Miyauchi Y, Ghosh R, Yoda M, Uchikawa S, Takito J, et al. The IRE1alpha-XBP1 pathway is essential for osteoblast differentiation through promoting transcription of Osterix. *EMBO reports*. 2011;12(5):451-7.
58. Jang WG, Kim EJ, Kim DK, Ryoo HM, Lee KB, Kim SH, et al. BMP2 protein regulates osteocalcin expression via Runx2-mediated Atf6 gene transcription. *The Journal of biological chemistry*. 2012;287(2):905-15.
59. Murakami T, Saito A, Hino S, Kondo S, Kanemoto S, Chihara K, et al. Signalling mediated by the endoplasmic reticulum stress transducer OASIS is involved in bone formation. *Nature cell biology*. 2009;11(10):1205-11.
60. Brown MS, Goldstein JL. The SREBP pathway: regulation of cholesterol metabolism by proteolysis of a membrane-bound transcription factor. *Cell*. 1997;89(3):331-40.
61. Brown MS, Goldstein JL. Cholesterol feedback: from Schoenheimer's bottle to Scap's MELADL. *Journal of lipid research*. 2009;50 Suppl:S15-27.
62. Eberle D, Hegarty B, Bossard P, Ferre P, Foufelle F. SREBP transcription factors: master regulators of lipid homeostasis. *Biochimie*. 2004;86(11):839-48.
63. Sakai J, Duncan EA, Rawson RB, Hua X, Brown MS, Goldstein JL. Sterol-regulated release of SREBP-2 from cell membranes requires two sequential cleavages, one within a transmembrane segment. *Cell*. 1996;85(7):1037-46.
64. Gorski JP, Huffman NT, Chittur S, Midura RJ, Black C, Oxford J, et al. Inhibition of proprotein convertase SKI-1 blocks transcription of key extracellular matrix genes regulating osteoblastic mineralization. *The Journal of biological chemistry*. 2011;286(3):1836-49.
65. Ting TC, Miyazaki-Anzai S, Masuda M, Levi M, Demer LL, Tintut Y, et al. Increased lipogenesis and stearate accelerate vascular calcification in calcifying vascular cells. *The Journal of biological chemistry*. 2011;286(27):23938-49.
66. Masuda M, Ting TC, Levi M, Saunders SJ, Miyazaki-Anzai S, Miyazaki M. Activating transcription factor 4 regulates stearate-induced vascular calcification. *Journal of lipid research*. 2012;53(8):1543-52.
67. Yoshida H, Matsui T, Yamamoto A, Okada T, Mori K. XBP1 mRNA is induced by ATF6 and spliced by IRE1 in response to ER stress to produce a highly active transcription factor. *Cell*. 2001;107(7):881-91.
68. Lisse TS, Thiele F, Fuchs H, Hans W, Przemeck GK, Abe K, et al. ER stress-mediated apoptosis in a new mouse model of osteogenesis imperfecta. *PLoS genetics*. 2008;4(2):e7.
69. Zhang C. Transcriptional regulation of bone formation by the osteoblast-specific transcription factor Osx. *Journal of orthopaedic surgery and research*. 2010;5:37.
70. Kohl S, Zobor D, Chiang WC, Weisschuh N, Staller J, Gonzalez Menendez I, et al. Mutations in the unfolded protein response regulator ATF6 cause the cone dysfunction disorder achromatopsia. *Nature genetics*. 2015;47(7):757-65.
71. DenBoer LM, Hardy-Smith PW, Hogan MR, Cockram GP, Audas TE, Lu R. Luman is capable of binding and activating transcription from the unfolded protein response element. *Biochemical and biophysical research communications*. 2005;331(1):113-9.

72. Brown MS, Ye J, Rawson RB, Goldstein JL. Regulated intramembrane proteolysis: a control mechanism conserved from bacteria to humans. *Cell*. 2000;100(4):391-8.
73. Chan CP, Kok KH, Jin DY. CREB3 subfamily transcription factors are not created equal: Recent insights from global analyses and animal models. *Cell & bioscience*. 2011;1(1):6.
74. Kondo S, Murakami T, Tatsumi K, Ogata M, Kanemoto S, Otori K, et al. OASIS, a CREB/ATF-family member, modulates UPR signalling in astrocytes. *Nature cell biology*. 2005;7(2):186-94.
75. Vellanki RN, Zhang L, Guney MA, Rocheleau JV, Gannon M, Volchuk A. OASIS/CREB3L1 induces expression of genes involved in extracellular matrix production but not classical endoplasmic reticulum stress response genes in pancreatic beta-cells. *Endocrinology*. 2010;151(9):4146-57.
76. Omori Y, Imai J, Watanabe M, Komatsu T, Suzuki Y, Kataoka K, et al. CREB-H: a novel mammalian transcription factor belonging to the CREB/ATF family and functioning via the box-B element with a liver-specific expression. *Nucleic acids research*. 2001;29(10):2154-62.
77. Zhang K, Shen X, Wu J, Sakaki K, Saunders T, Rutkowski DT, et al. Endoplasmic reticulum stress activates cleavage of CREBH to induce a systemic inflammatory response. *Cell*. 2006;124(3):587-99.
78. Lee MW, Chanda D, Yang J, Oh H, Kim SS, Yoon YS, et al. Regulation of hepatic gluconeogenesis by an ER-bound transcription factor, CREBH. *Cell metabolism*. 2010;11(4):331-9.
79. Zhang C, Wang G, Zheng Z, Maddipati KR, Zhang X, Dyson G, et al. Endoplasmic reticulum-tethered transcription factor cAMP responsive element-binding protein, hepatocyte specific, regulates hepatic lipogenesis, fatty acid oxidation, and lipolysis upon metabolic stress in mice. *Hepatology*. 2012;55(4):1070-82.
80. Barbosa S, Fasanella G, Carreira S, Llarena M, Fox R, Barreca C, et al. An orchestrated program regulating secretory pathway genes and cargos by the transmembrane transcription factor CREB-H. *Traffic*. 2013;14(4):382-98.
81. Jang WG, Jeong BC, Kim EJ, Choi H, Oh SH, Kim DK, et al. Cyclic AMP Response Element-binding Protein H (CREBH) Mediates the Inhibitory Actions of Tumor Necrosis Factor alpha in Osteoblast Differentiation by Stimulating Smad1 Degradation. *The Journal of biological chemistry*. 2015;290(21):13556-66.
82. Takahashi K, Yamanaka S. Induction of pluripotent stem cells from mouse embryonic and adult fibroblast cultures by defined factors. *Cell*. 2006;126(4):663-76.
83. Yu J, Vodyanik MA, Smuga-Otto K, Antosiewicz-Bourget J, Frane JL, Tian S, et al. Induced pluripotent stem cell lines derived from human somatic cells. *Science*. 2007;318(5858):1917-20.
84. Takahashi K, Tanabe K, Ohnuki M, Narita M, Ichisaka T, Tomoda K, et al. Induction of pluripotent stem cells from adult human fibroblasts by defined factors. *Cell*. 2007;131(5):861-72.
85. Shi Y, Inoue H, Wu JC, Yamanaka S. Induced pluripotent stem cell technology: a decade of progress. *Nature reviews Drug discovery*. 2017;16(2):115-30.
86. Deyle DR, Khan IF, Ren G, Wang PR, Kho J, Schwarze U, et al. Normal collagen and bone production by gene-targeted human osteogenesis imperfecta iPSCs.

- Molecular therapy : the journal of the American Society of Gene Therapy. 2012;20(1):204-13.
87. Belinsky GS, Ward L, Chung C. Pigment epithelium-derived factor (PEDF) normalizes matrix defects in iPSCs derived from Osteogenesis imperfecta Type VI. *Rare diseases*. 2016;4(1):e1212150.
  88. Gonzalez F, Boue S, Izpisua Belmonte JC. Methods for making induced pluripotent stem cells: reprogramming a la carte. *Nature reviews Genetics*. 2011;12(4):231-42.
  89. Okita K, Yamakawa T, Matsumura Y, Sato Y, Amano N, Watanabe A, et al. An efficient nonviral method to generate integration-free human-induced pluripotent stem cells from cord blood and peripheral blood cells. *Stem cells*. 2013;31(3):458-66.
  90. Okita K, Matsumura Y, Sato Y, Okada A, Morizane A, Okamoto S, et al. A more efficient method to generate integration-free human iPS cells. *Nature methods*. 2011;8(5):409-12.
  91. Mack AA, Kroboth S, Rajesh D, Wang WB. Generation of induced pluripotent stem cells from CD34+ cells across blood drawn from multiple donors with non-integrating episomal vectors. *PloS one*. 2011;6(11):e27956.
  92. Marti M, Mulero L, Pardo C, Morera C, Carrio M, Laricchia-Robbio L, et al. Characterization of pluripotent stem cells. *Nature protocols*. 2013;8(2):223-53.
  93. Hynes K, Menicanin D, Mrozik K, Gronthos S, Bartold PM. Generation of functional mesenchymal stem cells from different induced pluripotent stem cell lines. *Stem cells and development*. 2014;23(10):1084-96.
  94. Jaiswal N, Haynesworth SE, Caplan AI, Bruder SP. Osteogenic differentiation of purified, culture-expanded human mesenchymal stem cells in vitro. *Journal of cellular biochemistry*. 1997;64(2):295-312.
  95. Gregory CA, Gunn WG, Peister A, Prockop DJ. An Alizarin red-based assay of mineralization by adherent cells in culture: comparison with cetylpyridinium chloride extraction. *Analytical biochemistry*. 2004;329(1):77-84.
  96. Pruksananonda K, Rungsiwiwut R, Numchaisrika P, Ahnonkitpanit V, Isarasena N, Virutamasen P. Eighteen-year cryopreservation does not negatively affect the pluripotency of human embryos: evidence from embryonic stem cell derivation. *BioResearch open access*. 2012;1(4):166-73.
  97. Rungsiwiwut R, Ingrungruanglert P, Numchaisrika P, Virutamasen P, Phermthai T, Pruksananonda K. Human Umbilical Cord Blood-Derived Serum for Culturing the Supportive Feeder Cells of Human Pluripotent Stem Cell Lines. *Stem cells international*. 2016;2016:4626048.
  98. Moraes DA, Sibov TT, Pavon LF, Alvim PQ, Bonadio RS, Da Silva JR, et al. A reduction in CD90 (THY-1) expression results in increased differentiation of mesenchymal stromal cells. *Stem cell research & therapy*. 2016;7(1):97.
  99. Sodek J, Chen J, Nagata T, Kasugai S, Todescan R, Jr., Li IW, et al. Regulation of osteopontin expression in osteoblasts. *Annals of the New York Academy of Sciences*. 1995;760:223-41.
  100. Termine JD, Kleinman HK, Whitson SW, Conn KM, McGarvey ML, Martin GR. Osteonectin, a bone-specific protein linking mineral to collagen. *Cell*. 1981;26(1 Pt 1):99-105.



101. Delany AM, Kalajzic I, Bradshaw AD, Sage EH, Canalis E. Osteonectin-null mutation compromises osteoblast formation, maturation, and survival. *Endocrinology*. 2003;144(6):2588-96.
102. Reich A, Bae AS, Barnes AM, Cabral WA, Hinek A, Stimec J, et al. Type V OI primary osteoblasts display increased mineralization despite decreased COL1A1 expression. *The Journal of clinical endocrinology and metabolism*. 2015;100(2):E325-32.



**APPENDIX**



จุฬาลงกรณ์มหาวิทยาลัย  
**CHULALONGKORN UNIVERSITY**

**VITA**

Name Miss Siraprapa Tongkobpetch

Date of birth September 2nd, 1979

Place of birth Bangkok, Thailand

**Education**

1997-2000 B.Sc., Genetic sciences, Department of Botany, Faculty of Science, Chulalongkorn University, Bangkok, Thailand

2002-2004 M.Sc., Medical sciences, Faculty of Medicine, Chulalongkorn University, Bangkok, Thailand

2011-2017 Ph.D., Student in Biomedical Sciences program, Faculty of Graduate School, Chulalongkorn University, Bangkok, Thailand

**Scholarship**

2011-2017 The Royal Golden Jubilee Ph.D. Program.